



# Assessment of the performance of CORDEX-SA experiments in simulating seasonal mean temperature over the Himalayan region for the present climate: Part I

T. Nengker<sup>1</sup> · A. Choudhary<sup>1</sup> · A. P. Dimri<sup>1</sup>

Received: 11 May 2016 / Accepted: 19 February 2017 / Published online: 15 March 2017  
© Springer-Verlag Berlin Heidelberg 2017

**Abstract** The ability of an ensemble of five regional climate models (hereafter RCMs) under Coordinated Regional Climate Downscaling Experiments-South Asia (hereafter, CORDEX-SA) in simulating the key features of present day near surface mean air temperature ( $T_{\text{mean}}$ ) climatology (1970–2005) over the Himalayan region is studied. The purpose of this paper is to understand the consistency in the performance of models across the ensemble, space and seasons. For this a number of statistical measures like trend, correlation, variance, probability distribution function etc. are applied to evaluate the performance of models against observation and simultaneously the underlying uncertainties between them for four different seasons. The most evident finding from the study is the presence of a large cold bias ( $-6$  to  $-8^{\circ}\text{C}$ ) which is systematically seen across all the models and across space and time over the Himalayan region. However, these RCMs with its fine resolution perform extremely well in capturing the spatial distribution of the temperature features as indicated by a consistently high spatial correlation (greater than 0.9) with the observation in all seasons. In spite of underestimation in simulated temperature and general intensification of cold bias with increasing elevation the models show a greater rate of warming than the observation throughout entire altitudinal stretch of study region. During winter, the simulated rate of warming gets even higher at high altitudes. Moreover,

a seasonal response of model performance and its spatial variability to elevation is found.

**Keywords** RCMs · CORDEX-SA · Himalayan region · Temperature · Climatology · Seasonal · Cold bias · Elevation

## 1 Introduction

The assessment reports of IPCC (IPCC 2007, 2014) highlights that human activities related with emission of greenhouse gases are responsible for more than 90% of the climate warming across the globe which has happened since 1950s. The future projections also suggest that there will be a significant accelerated rate of warming in twenty-first century compared with what has already been observed in twentieth century (Ruosteenoja et al. 2003). In such a global warming scenario, mountain environments are thought to be more susceptible to climate change due to their complex topography which is related with causing rapid and systematic changes in climatic parameters in response to radiative forcings (Xu et al. 2009). Temperature, besides, precipitation, is one of the most sensitive parameters, which is variable at very short spatial scales in mountains (Becker 1997). Therefore, the mountain systems are considered to be interesting study areas for early detection of the signals of changing climate and also its impacts on associated systems—hydrology, economy and society (Beniston 2003). The Himalayan region with an average height of 4000 m (Rangwala and Miller 2012) is abode to some of the highest mountain summits of the world such as Mount Everest (8850 m), Karakoram (8611 m), Kanchenjunga (8586 m) etc. It has been described as one of the regions

**Electronic supplementary material** The online version of this article (doi:[10.1007/s00382-017-3597-x](https://doi.org/10.1007/s00382-017-3597-x)) contains supplementary material, which is available to authorized users.

✉ A. P. Dimri  
apdimri@hotmail.com

<sup>1</sup> School of Environmental Sciences, Jawaharlal Nehru University, New Delhi 110067, India

that are significantly vulnerable to the impacts of climate change (Xu et al. 2009). This is because the Himalayas is the largest ice-covered region on the surface of Earth outside the two poles and their glaciers form the source of major South Asian rivers like Indus, Ganges, Brahmaputra etc. More than a billion people living in these river basins depend on them for water and highly fertile land which is required for agriculture—the mainstay of the socio-economic structure of the South Asian countries (Gautam et al. 2009). Any abnormal change in climatic parameters would pose a serious threat to the sustainability of life in this part of world (Barnett et al. 2005).

With this importance of the region, there are only a few studies to assess the projections of climatic parameters especially temperature and precipitation (Panday et al. 2015). This is mainly because of the complex and inaccessible topography and harsh climate of the region where the existing meteorological stations are very scarce especially at the higher elevations so the data provided by them tend to have biases for high altitudes as most of the stations are located in valleys which are under representative for the whole area (Fowler and Archer 2006; Winiger et al. 2005). Besides, the observation being available for only a few variables there also exist uncertainties between various observational datasets due to different gridding techniques (Hofstra et al. 2008), data quality issues like low station density (Schmidli et al. 2001) or uneven allocation of stations (Haslinger et al. 2013). Mishra (2015) in his study over the Himalayan region using a set of gridded observational datasets for temperature found an uncertainty in these datasets to be as high as 0.2–0.5 °C during winter and monsoon, respectively. Therefore, understanding the climatic processes taking place at the basin level and its hydrology becomes difficult. This underlines the need of also using climate models. While global climate models (GCMs) have a very coarse resolution which deems it unsuitable to simulate the climate of a highly complex topographic region (Kumar et al. 2013), the regional climate models (RCMs) on the other hand, due to the representation of fine scale processes and topography in its physics, present an opportunity to capture the sub-grid scale processes—local climatic forcing and feedbacks in a region like Himalaya (Giorgi and Bates 1989; Beniston 2003; Dimri 2009; Rummukainen 2010). However, it is simultaneously important to evaluate the RCMs against observational dataset for their performance in simulating the climatic variables in the Himalayan region. As the study of climate change, its impact and vulnerability assessment based on different warming scenarios have increased in the last decade (Lobell et al. 2007; Mote et al. 2011), and use of multi-model data is going to increase in future (Overpeck et al. 2011), an analysis of existing model data i.e. the evaluation of model for the present climate and the

uncertainty existing within the set of models thus needs to be studied.

Temperature is a very important indicator of climate change. Also it is a major driver of various energy exchange processes occurring in the atmosphere and on land which involves the transfer of mass and heat as it represents the thermodynamic state of the system (Winnikov et al. 1990; Thapliyal and Kulshrestha 1991). Therefore any significant change in temperature over the Himalayan region can cause a critical shift in the climatic patterns including hydrological and glacial settings. Past studies confirm a clear picture of consistently increasing temperature over the Himalayan region (Liu and Chen 2000; Shrestha et al. 1999, 2000; Shekhar et al. 2010; Dimri and Dash 2012). Future projections also suggest that warming will be significant over the Himalayans, including the Tibetan Plateau (Gao et al. 2003). Tibetan Plateau could warm by 2.5 °C by 2050 and 5 °C by 2100 (Rupa Kumar et al. 2006). Various works have suggested that warming in the Himalayas is much greater than the global average of 0.74 °C over the last century (IPCC 2007; Du et al. 2004). For example, Shrestha et al. (1999) reported warming of 0.6 °C per decade between 1977 and 2000 over Nepal. Immerzeel (2008) found that in eastern Himalaya and Tibetan Plateau over Brahmaputra basin a basin-wide warming trend similar to global average temperature 0.6 °C/100 year exists for the period 1901–2002. In another study, 1.6 °C warming in the last century is reported over north-western Himalayan region by Bhutiyani et al. (2007). In a recent study based on Climatic Research Unit's reconstructed temperature dataset it was found that the Himalayas and Tibet Plateau have warmed at a higher rate in the last few decades than that in the last century (Diodato et al. 2012). Dash et al. (2007) reported that western Himalayas warmed by over 0.9 °C during 1901–2003.

Season specific responses to warming is also reported over the Himalayans. The warming rate is found to be consistently higher in winter compared with other seasons in most parts of the Himalayas, namely, the Chinese, north-west Indian, and Nepalese Himalaya (Bhutiyani et al. 2007; Shrestha et al. 1999; Shrestha and Devkota 2010). For example, Dimri and Dash (2012) found increasing trend of temperature over the western Himalayas based on winter (December–February) records from 1975 to 2006 with highest trend observed for maximum temperature. Over the same region, Yadav et al. (2004) reported pre-monsoon cooling (March–May). Singh et al. (2008) reported an increasing trend of seasonal average daily maximum temperature for all seasons except monsoon in lower Indus basin. Tse-ring et al. (2012) found an increase of 0.5 °C in mean temperature during non-monsoon season over Himalayan regions in Bhutan from 1985 to 2002. Gautam et al. (2009) reported an enhancement of pre-monsoon warming

during 1979–2007. Fowler and Archer (2005) and Khattak et al. (2011) found a warming trend in winter temperature between 1961 and 2000 and 1967–2005 respectively in upper Indus basin. The seasonal dependent trend of warming with greatest warming in winter season and smallest in summer has also been found by researchers in Tibetan Plateau (e.g. Du et al. 2004; Liu and Chen 2000; You et al. 2008).

Recent studies have also shown that in regions of complex topography such as the Himalayas and other mountainous regions across the world, a dependency of trends on elevation in temperature has been seen which could be more apparent in tropical regions (Beniston and Rebetez 1996; Beniston et al. 1997; Diaz and Bradley 1997; Liu and Chen 2000; Diaz et al. 2003; Liu et al. 2009; You et al. 2010; Rangwala and Miller 2012; Pepin et al. 2015). New et al. (2002) found that warming in the Nepal and Tibet has shown a progressively greater trend with elevation and even suggested that the pattern of higher rate of warming with higher elevation is prevalent over entire greater Himalayan region. Some specific studies over the Himalayas in Xizang province of China found higher warming trends at higher altitudes (Liu et al. 2009; Liu and Chen 2000; Qin et al. 2009). However, there are studies which report greater warming trends at lower elevations (Vuille and Bradley 2000; Pepin and Losleben 2002; Lu et al. 2010). In addition, there are studies where not any dependency of warming with elevation is found at all (Vuille et al. 2003; Pepin and Lundquist 2008; You et al. 2010). Also some studies report discrepancies within the same region of mountain having different relationship of warming with elevation.

The climatic response variation with elevation could be explained by several reasons—such as snow/ice albedo feedback, presence of aerosol (Lau et al. 2010), cloud cover changes (Sun et al. 2000), changes in surface energy balance, soil moisture and humidity changes etc. (Rangwala and Miller 2012) but still the mountain environment are inherently difficult to understand because of their complex physiography which is a challenging task to represent accurately in climate models. Due to extreme topographic variability and landuse heterogeneity over the Himalayas and the complex climatic response to greenhouse gas forcings, even the high resolution RCMs fail to give reliable projections of climate change over the Himalayas. But still, to understand comprehensively the process and mechanism of climatic changes over inaccessible areas like the Himalayas and to study the future implications of climate change, RCMs are the best tool in hand provided they are bench tested against high quality observational datasets. This is required because models tend to have biases (cold or warm) and uncertainties. Further a single climate model cannot be relied upon for its accuracy therefore; the use of multi-model ensembles not only provides information about

differences among model projections but also provides an opportunity to understand the regional behaviour of climatology across models and scenarios.

There are only a few studies in the past where the model is used for simulating regional temperature climatology over a complex terrain such as the mountains. Giorgi and Bates (1989) used a mesoscale model to simulate the climate over complex terrain in south-west US. They found the model showing cold bias of about 1–2 °C in entire lower troposphere. In a similar study over Greater Alpine region, Haslinger et al. (2013) also reported a cold bias in COSMO-CLM regional model. They attributed the underestimation of temperature by model to its wet bias in precipitation which leads to cold bias in temperature due to snow cover, moisture and evaporation feedbacks. They also reported the cold bias to have a dependence on elevation with an intensification with increasing height. The bias was found to have seasonal variation with maximum cold bias in winter season. They also found the model trend to be contradictory to observation as the model exhibited a weaker trend with positive values at higher altitudes and negative at lower elevations. The cold bias in RCMs in mountainous regions is common feature as noted in several other studies (Giorgi et al. 2004; Solomon et al. 2008). Over the Himalayan region, Akhtar et al. (2009) in his study reported a cold bias in the regional model—PRECIS and related it with the bias in the GCM forcings. Colder bias may suggest that there is a larger/smaller nighttime/daytime surface sensible heat flux in the model compared with reality or less vertical mixing of heat. In a very recent study, by Mishra (2015) using a set of RCMs under CORDEX project, an intense cold bias of upto 6–8 °C was found in the models. Also a large uncertainty between the models was found in simulating the temperature. He explained the cause for this to be the different topographic representation of Himalaya region in different RCMs.

Most of the past studies over mountain regions are carried out either using a single or a few RCMs—a factor which has significant influence on the internal variability of model at shorter time scales (Vanvyve et al. 2008). Therefore, in the past few years, significant efforts are made across the globe to establish frameworks in form of coordinated efforts to use several RCMs aimed at improving the characterization of regional climate. Though, a major limit to such studies is that there is little coherency in designing the project and coordination (Giorgi et al. 2008; Gbobaniyi et al. 2011). This lack of uniformity in the models and their output limits the utilization of the model to the community of regional modelers and of data to the end users. The Coordinated Regional Climate Downscaling Experiment (CORDEX) is one of a global initiative by the World Climate Research Programme (WCRP) which aims to coordinate international effort in regional climate

downscaling and improve on lessons learnt from previous projects (Giorgi et al. 2009; Evans 2011; Jones et al. 2011). CORDEX regions of interest or domains encompass almost all of the planet's inhabited landmass and also the poles. In the present study, we will be focusing on Himalayan region which lies in South Asia domain of CORDEX domain (hereafter CORDEX-SA). Ghimire et al. (2015) analyzed the CORDEX-SA simulations for the present climate (1970–2005) over the Himalayan region. In that study, the authors focused only on precipitation variable for the evaluation of model climatology and variability. So, in the present work, we extend that study for analysis of mean temperature (2 m) climatology and related characteristics to assess the performance of CORDEX-SA models. We aim to find how the model performance varies with each other and across the length and breadth of the Himalayan region along with its dependency on altitudinal and seasonal changes. We intend to bring out from our analysis the major shortcomings in models in comparison with observation as well as their skills and propose the possible reasons behind such behaviours.

Thus, in the present study we tried to assess the performance of individual models (or experiments, used interchangeably hereafter) under CORDEX-SA as well as their intercomparison for two basic reasons. First, that these CORDEX models are currently in focus and are being used widely around the world, so unless we assess the

performance of models, end-users of the CORDEX data cannot rely on the information provided by these models. Second, unless we bring forth the particular strengths and weaknesses of models the model developers cannot build on it for work on subsequent improvement of respective models. But we would also like to emphasize that if a particular model is showing good/poor skill in simulating the temperature over the Himalayan region does not mean that it will perform the same over other mountain regions or for that matter for any other variable.

The paper is organized as follows. Section 2 describes the data and methodology used in the analysis. Section 3 reports and discusses the results of the analyses in terms of observed and model climatology, the bias in the models and its altitudinal distribution, annual cycle, yearly variability, the long-term trends and its variation with elevation, time series, inter-model spread, spatial correlation and probability distribution function. Finally, in Sect. 4 we conclude by presenting our main findings.

## 2 Data and methodology

### 2.1 Study region

The study region includes the great Himalayan Range along with the Hindu-Kush and the Karakoram, as shown

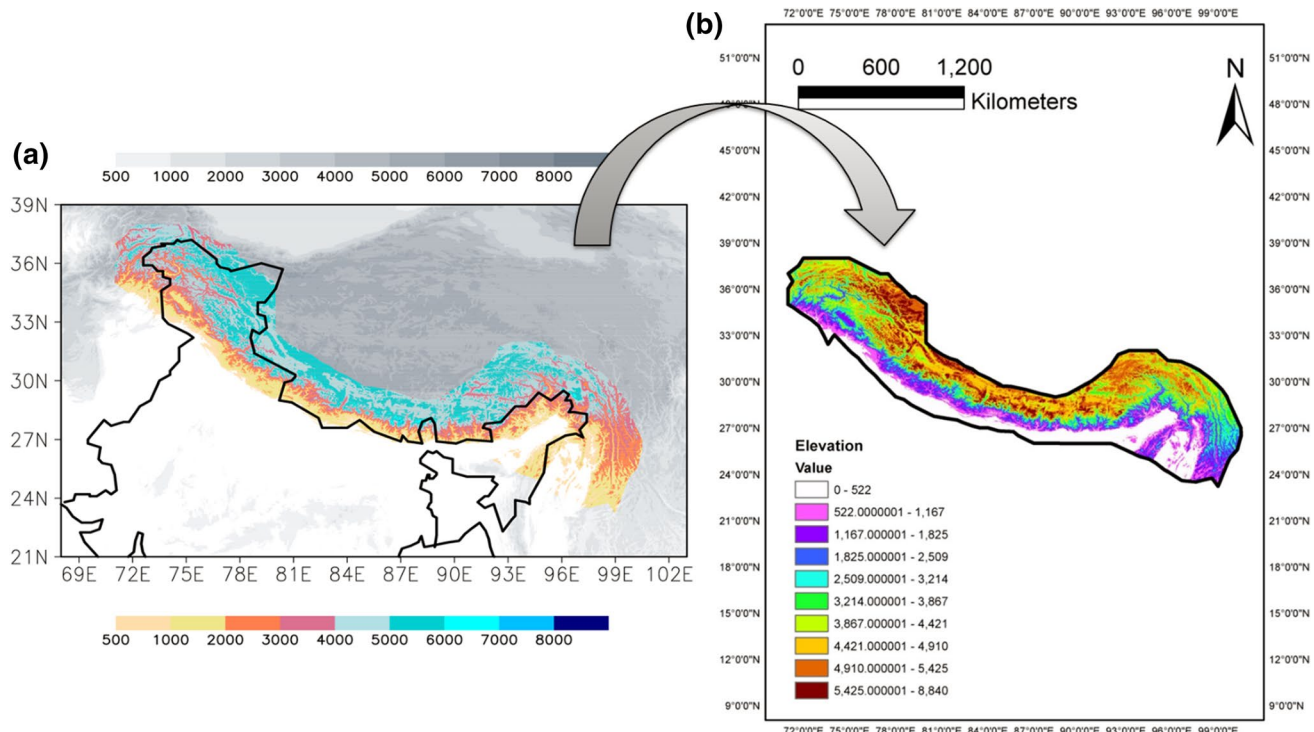


**Fig. 1** Topography (m) over **a** Himalayan and Tibetan region (m, grey shaded) and over **b** study area (m, color shaded) (Ghimire et al. 2015)

in Fig. 1a. It is often referred to as the “third pole” (Qiu 2008) of Earth. Along the southern margin of the Tibetan plateau, the great Himalayan Range covers about 2500 km from the west to the east which acts as a barrier between the tropical and polar air masses (Nieuwolt 1977). The Himalayas owns the biggest mountain chains of the Earth with largest ice mass apart from the Polar Regions. The tropical location makes the Himalayas to be one of the most sensitive indicators of climate change (IPCC 2007). Diverse climatic, hydrological and ecological traits of the Himalayas are attributed to its geographical setting. From tropical to Alpine, distinct climatic conditions prevail within the region with respect to the changing altitude (Kulkarni et al. 2013). However, according to Immerzeel et al. (2009), Shrestha et al. (2000) and Pellicciotti et al. (2012), there is still an acute limitation in the details of climatology of the region which necessitates in taking up this study.

Our study region extends from 23° to 39°N and 68° to 103°E, which is distinguished from the surrounding elevations using colours as shown in Fig. 1a (Ghimire et al. 2015). The region covers parts of eight countries from Tajikistan in west to Myanmar in east including Afghanistan, Pakistan, India, Nepal, Bhutan and southern China (Palazzi et al. 2013). In Fig. 1b our study region is further differentiated based on varying elevations.

## 2.2 Data

### 2.2.1 CORDEX experiments or model data

Coordinated Regional Climate Downscaling Experiment (CORDEX) project under World Climate Research Program (WCRP) aims to lead an international coordinated framework to develop an improved projection of climate change at the regional scale. This program was initiated to study the regional climate change scenarios globally (Fernández et al. 2010; Giorgi et al. 2009). 5 combinations of various RCMs with initial and boundary conditions forcings from different GCMs (refer to Table 1 for the name of the experiments and other details) comprises the CORDEX South Asia (CORDEX-SA) domain experiments considered in the present study. The CORDEX-SA data used is available at a spatial resolution of 0.44° (approximately 50 km) at daily temporal resolution.

The near-surface (2 m) mean air temperature or ( $T_{\text{mean}}$ , used interchangeably hereafter) data for the CORDEX-SA was originally obtained from Center for Climate Change Research (CCCR), Indian Institute of Tropical Meteorology (IITM), Pune, India which maintains the database and is also the coordinating institution of CORDEX-SA.

**Table 1** CORDEX experiment details. (Source: CORDEX South-Asia Database, CCCR, IITM <http://ccer.tropmet.res.in/cordex/files/downloads.jsp>)

S. No.	Experiment name	Name used	RCM description	Driving GCM	Contributing institute
1	LMDZ-IITM-RegCM4	LMDZ	The Abdus Salam International Centre for Theoretical Physics (ICTP) Regional Climatic Model version 4 (RegCM4; Giorgi et al. 2012)	IPLS LMDZ4	CCCR, IITM
2	GFDL-ESM2M-IITM-RegCM4	GFDL	ICTP RegCM4	Geophysical Fluid Dynamics Laboratory, USA, Earth System Model (GFDL-ESM2M-LR; Dunne et al. 2012)	CCCR, IITM
3	ICHEC-EC-EARTH-RCA4	ICHEC	Rossby Centre regional atmospheric model version 4 (RCA4; Samuelsson et al. 2011)	Irish Centre for High-End Computing (ICHEC), European Consortium ESM (EC-EARTH; Hazeleger et al. 2012)	Rossby Centre, Swedish Meteorological and Hydrological Institute (SMHI), Sweden
4	COSMO-CLM	COSMO-CLM	COnsortium for Small-scale MOdelling (COSMO) model in CLimate Mode version 4.8 (CCLM; Dobler and Ahrens 2008)	Max Planck Institute for Meteorology, Germany, Earth System Model (MPI-ESM-LR; Giorgi et al. 2013)	Institute for Atmospheric and Environmental Sciences (IAES), Goethe University, Frankfurt am Main (GUF), Germany
5	MPI-ESM-LR-REMO2009	REMO	REMO	MPI Regional model 2009 (Saeed et al. 2012)	Climate Service Center, Hamburg, Germany

## 2.2.2 Observational data

Lack of long term weather records has limited the analyses of climatic trends over the Himalayas (Shrestha and Aryal 2011). Further, the topography induced inaccessibility and sparse distribution of meteorological stations across the Himalayan region contributes towards the highly non-homogeneous characteristic of available data. The complex terrain can enhance differences in climate even over short distances which can have significant impact on spatial variability. In such cases, long-term gridded temperature datasets cater the potential to deduce values and climatic information that station data could not capture. However, existing gridded datasets generally do not give the most reliable estimations of long-term trends since stations are distributed heterogeneously over a vast geographical area and have varying record lengths. Hence artificial trends can be introduced during the gridding procedure (Hamlet and Lettenmaier 2005). Moreover, there exists an observational uncertainty between the gridded datasets which is very important to be assessed before selecting a particular datasets for model evaluation which we have done in this study. Over a complex terrain such as the Himalayas, where we can have a highly variable vertical profile of a climatic parameter such as temperature, the observational uncertainties could be even higher (Stahl et al. 2006; Daly 2006). Sources of these uncertainties in the observational datasets could emerge from different gridding methods applied (Hofstra et al. 2008; Ensor and Robeson 2008) or data quality issues (Schmidli et al. 2001). Low station density, uneven apportioning of stations and finally the alteration of station density over time can influence the estimates of grid-point average by affecting the variance (Hofstra et al. 2010; Perry and Hollis 2005).

In our study, we have firstly tried to assess the uncertainty in observations by carrying a comparative study of  $T_{\text{mean}}$  climatology for the present climate between using following four gridded observational datasets:

1. Asian Temperature Dataset (APHROTEMP, Version: V1204R1, Yasutomi et al. 2011).
2. Climatic Research Unit (CRU, Version: TS (time-series) 3.22, Harris et al. 2014a, b).
3. University of Delaware (UDW, Version 3.01, Matsuura et al. 2012)
4. National Centers for Environmental Prediction Reanalysis (NCEP; Kalnay et al. 1996).

Asian Temperature Dataset available at two different spatial resolutions  $0.25^{\circ}$  and  $0.5^{\circ}$ , Climatic Research Unit (hereafter, CRU) data and University of Delaware (hereafter, UDW) data with spatial resolution of  $0.5^{\circ}$  and National Center for Environmental Prediction (hereafter, NCEP)

reanalysis data with  $1.87^{\circ}$  spatial resolution for the period of 1970–2005 are considered. This period is selected to maintain consistency with all the observation datasets as well as the models as this was the common period for which the data was available from all the models.

The daily mean gridded surface temperature data APHROTEMP (version: V1204R1) was developed under the APHRODITE project using collection of observed temperature data from the station measurements for Monsoon Asia (Yasutomi et al. 2011). An advanced interpolation technique has been used to prepare this dataset in which quality controlled observations from over 5000 to 12,000 station data was converted into the gridded form by methods as described in (Yatagai et al. 2012; Xie et al. 2007; Willmott et al. 1985). The high resolution ( $0.5^{\circ}$ ) near-surface temperature gridded dataset CRU time-series (TS) Version 3.22 was produced by the Climatic Research Unit at University of East Anglia, UK. An archive of daily mean, maximum and minimum temperature datasets was prepared by collecting data from more than 4000 weather stations around the world (Harris et al. 2014a, b). The UDW gridded temperature dataset was constructed by collecting data from over 1600 to 12,300 stations which were interpolated to  $0.5^{\circ}$ . The data comes from several updated sources including a recent version of the Global Historical Climatology Network (GHCN2), (Peterson et al. 1998), the Global Synoptic Climatology Network (Dataset 9290c, courtesy of National Climatic Data Center), Global Surface Summary of Day (GSOD) (NCDC) etc. by using a combination of spatial interpolation methods as described in (Willmott and Matsuura 1995; Willmott et al. 1985; Willmott and Robeson 1995; Matsuura and Willmott 2009). Various studies are carried out using this dataset (Bond-Lamberty and Thomson 2010).

There is a need to further select one observational dataset as a reference for model evaluation. This final observational dataset is selected on the basis of robustness of its algorithm by which it is prepared and its previous uses which makes it most suitable for further evaluation over the study region. In this study, APHROTEMP at  $0.5^{\circ}$  resolution (hereafter APHROTEMP 0.5 or simply APHROTEMP) is further used for the performance evaluation of CORDEX-SA experiments and their inter-comparison. APHROTEMP, developed under Asian Precipitation-Highly-Resolved Observational Data Integration Towards Evaluation's (APHRODITE) Water resources project over 'Monsoon Asia' domain, is the only product in Asia that has high resolution both spatially and temporally (Yasutomi et al. 2011). It is the only long-term (1961 onward) continental-scale daily temperature product that is constructed from a dense network of daily weather data for Asia which includes the Himalayas, South and Southeast Asia and mountainous areas in the Middle East (Yatagai et al.

2009, 2010; Hamada et al. 2011). The number of stations (5000–12,000) is up to 1.5–3 times higher than the stations based on global telecommunication system (GTS) networks used to develop other temperature products. It is developed using an automated quality control (QC) system to detect erroneous temperature data. APHROTEMP provides a higher quality temperature dataset than UDW and CRU for Indian summer and winter, credits to its higher station density and robust algorithm of conversion to gridded form. This dataset is also used for monitoring long-term changes and statistical analysis of extreme weather (Yasutomi et al. 2011). The use of APHROTEMP dataset is rapidly increasing for impact studies over the Monsoon Asia region (Madhura et al. 2015; Duncan et al. 2015) and to study the climatic uncertainties over the Himalayas (Mishra 2015).

### 2.3 Methodology

The evaluation of models is carried out for different seasons because each season exhibits distinct climatic conditions and the skill of models vary accordingly because the internal dynamics of a model is very sensitive to the prevailing atmospheric conditions. Therefore, we carried out the study for all the four seasons of the region i.e. winter (DJF), pre-monsoon (MAM), monsoon (JJAS) and post-monsoon (ON) to see how well models represent the seasonal transition and to see if the model dynamics perform better in any particular season.

Firstly, for the evaluation of model performance in simulating temperature climatology, first step was to select a common timeframe based on the availability of data for each CORDEX-SA experiment and the reference dataset APHROTEMP. Hence, the period 1970–2005 was chosen for the convenience of the study. The other reason to choose this period is to evaluate how well the models represent the present climate change as monotonous rising trends have been observed after 1970 in the global and regional records of temperature. Prior to this period descending trend was observed (Jones and Mann 2004; Shrestha et al. 2000). The RCM data used in the study produced by different modelling groups and driven by different GCMs so they vary in their native grid structure and format. So, there is a need to bring all the model datasets along with the reference observational dataset into a common data format and grid resolution of  $0.5^{\circ}$  to carry out comparative studies. For this analysis, a climate data post processing tool called climate data operators (CDO) is used (Schulzweida et al. 2006). The same tool i.e. CDO is used to mask out the CORDEX-SA data for the study region i.e. the Himalayas from the original file which covered the entire South Asia domain. The study region encompasses about 473 gridpoints at  $0.5^{\circ}$  resolution.

Comparison between the observed and simulated seasonal  $T_{\text{mean}}$  climatology including the bias of latter is studied to assess the performance of models in capturing the space dependent long-term time mean of temperature. Simultaneously, the inter comparison of different models would give an idea of uncertainty present between them. We also studied the annual cycle of  $T_{\text{mean}}$  averaged over the study area (shown in Fig. 1) to see whether the models are able to simulate the  $T_{\text{mean}}$  seasonality. Analysis of trend (1970–2005) is also discussed to understand the ability of models to simulate temporal variability and long-term change in seasonal mean temperature along with its spatial distribution. This gives us an understanding of how various external forcings can affect trend simulation by models (Giorgi et al. 2004). The rate of change or the slope existing in the year wise seasonal mean temperature values is calculated by applying least square regression method. Further, season wise altitudinal distribution of trend, climatology, climatology bias and trend difference between model and observation to get an insight of their relationship with topography in the complex terrain is also studied.

To make the model evaluation more robust, other statistical procedures like spatial correlation (Pearson correlation coefficient; Hall 2015), inter-model standard deviation and Taylor diagram analysis is applied. Inter-model standard deviation or ensemble spread aids in understanding the degree of uncertainty or agreement between the different model simulations. The Taylor diagram, through a single picture gives a graphical representation of the extent of spread between models and with the observation in terms of their spatial correlation, centered root mean square (RMS) difference and the spatial variance which is represented by their standard deviation (Taylor 2001, 2005). Finally, to assess the ability of RCMs in representing the whole range of temperature distribution over the study region, we compared the frequency distribution of simulated temperature with that of observation as fitted normal or Gaussian probability distribution function (PDF). The PDFs of the temperature follows the Gaussian distribution (Wilks 2011; Fan et al. 2014, 2015) as:

$$f(x|\mu, \sigma) = \frac{1}{\sigma \sqrt{2\pi}} e^{-\frac{1}{2} \left( \frac{x-\mu}{\sigma} \right)^2},$$

where  $\mu$  is the mean of temperature distribution and  $\sigma$  is the standard deviation of the temperature distribution.

### 3 Results and discussion

In Fig. 2, we compare the  $T_{\text{mean}}$  climatology of different observations for all the seasons (DJF, MAM, JJAS and ON) for the time period 1970–2005. The temperature

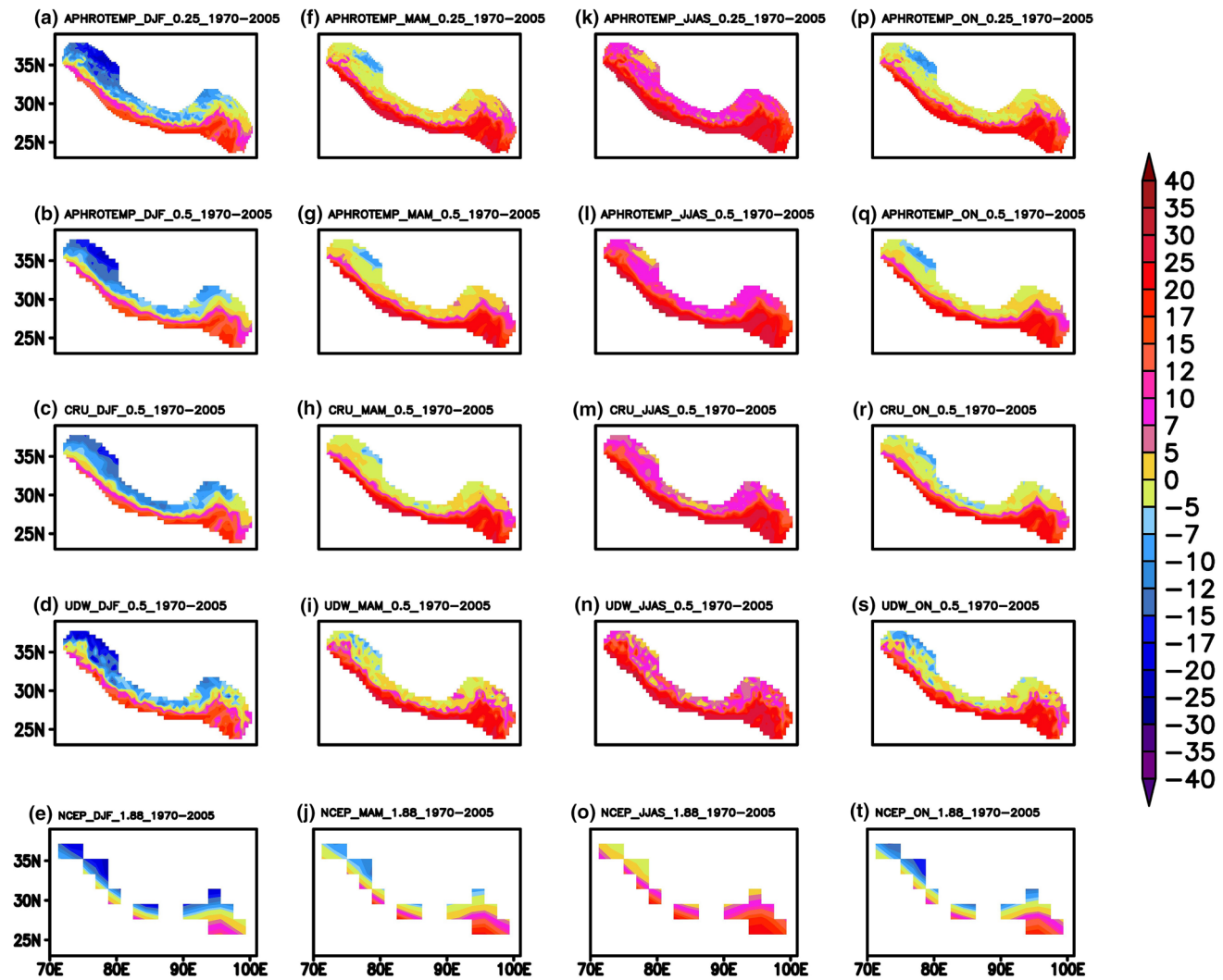


**Fig. 2** Observed seasonal mean temperature,  $T_{\text{mean}}$  ( $^{\circ}\text{C}$ ) climatology during 1970–2005 over the study area. *First column corresponds to winter (DJF); second column corresponds to pre-monsoon (MAM), third column corresponds to monsoon (JJAS) and last column corresponds to post-monsoon (ON)*

climatology captured by observations reflects the topography and natural climatic setting of the Himalayas. The observations also show the seasonal variations in temperature. The temperature distribution in all the observation datasets follows the topography over the Himalaya (as shown in Fig. 1), with the lower elevation region along the foothills and the south-eastern Himalaya displaying the higher temperature while the higher reaches of the Himalayas above the foothills all along the study region from west to east shows lower temperature. This indicates the role of orography as well as the slope environmental lapse rate on the temperature distribution (Thayyen and Dimri 2014). Variables like topography (exposure and aspect) and slope are the factors responsible for the microclimate of the mountains. However, similar to the observations by Wiltshire (2014), Fig. 2, we can see that due to latitudinal

and surface property differences, the northwestern Himalayas (Karakoram) shows colder temperature than the Central Himalaya (Nepal, Bhutan) despite being at similar elevation (refer Fig. 1). Sharp gradient in the spatial distribution of  $T_{\text{mean}}$  is seen in all the observations, though with very slight differences. Further, the seasonal variation in temperature is also well represented in all the observations with gradual intensification of warming from DJF (winter) to highest temperature in JJAS (monsoon) season. In the JJAS, even the higher altitudes exhibit higher temperature, above  $0^{\circ}\text{C}$  across the study region. Following the topography, the temperature climatology of APHROTEMP 0.5 (second row from top) for different seasons ranges from  $-20$  to  $+25^{\circ}\text{C}$  for DJF (winter),  $-10$  to  $+30^{\circ}\text{C}$  for MAM (pre-monsoon),  $5$ – $35^{\circ}\text{C}$  for JJAS (monsoon) and  $-20$  to  $+20^{\circ}\text{C}$  for ON (post-monsoon). In the NCEP dataset (last

row, Fig. 2), the pattern discussed above is though seen but not so evidently portrayed due to very coarse resolution. The uncertainty between the observational datasets is not very significant as far as the climatological distribution is concerned although the magnitudes vary significantly.

As we have discussed already, APHROTEMP 0.5 represents the temperature distribution well over the region with a clear band of higher temperature along the southern rim of the Himalayas extending up to south-east India and the general lower temperature as we move towards the northwest. Following Yatagai et al. (2009) and Krishnamurti et al. (2009), availability of high station density during the preparation of this regressed temperature dataset

and better representation of vertical and horizontal gradient made us to select APHROTEMP 0.5 as the reference dataset for evaluation and comparison of the experiments. APHROTEMP 0.25 despite having better resolution than APHROTEMP 0.5, was not chosen as the reference because the CORDEX-SA model data are available at a resolution of  $0.5^{\circ}$ .

Figure 3 shows the simulated seasonal  $T_{\text{mean}}$  climatology over the study region for the CORDEX-SA experiments (top four rows) and their ensemble mean (last row, hereafter ENSEMBLE). Though the models tend to show differences in temperature from the observation, which will be discussed further in bias study, but in general the

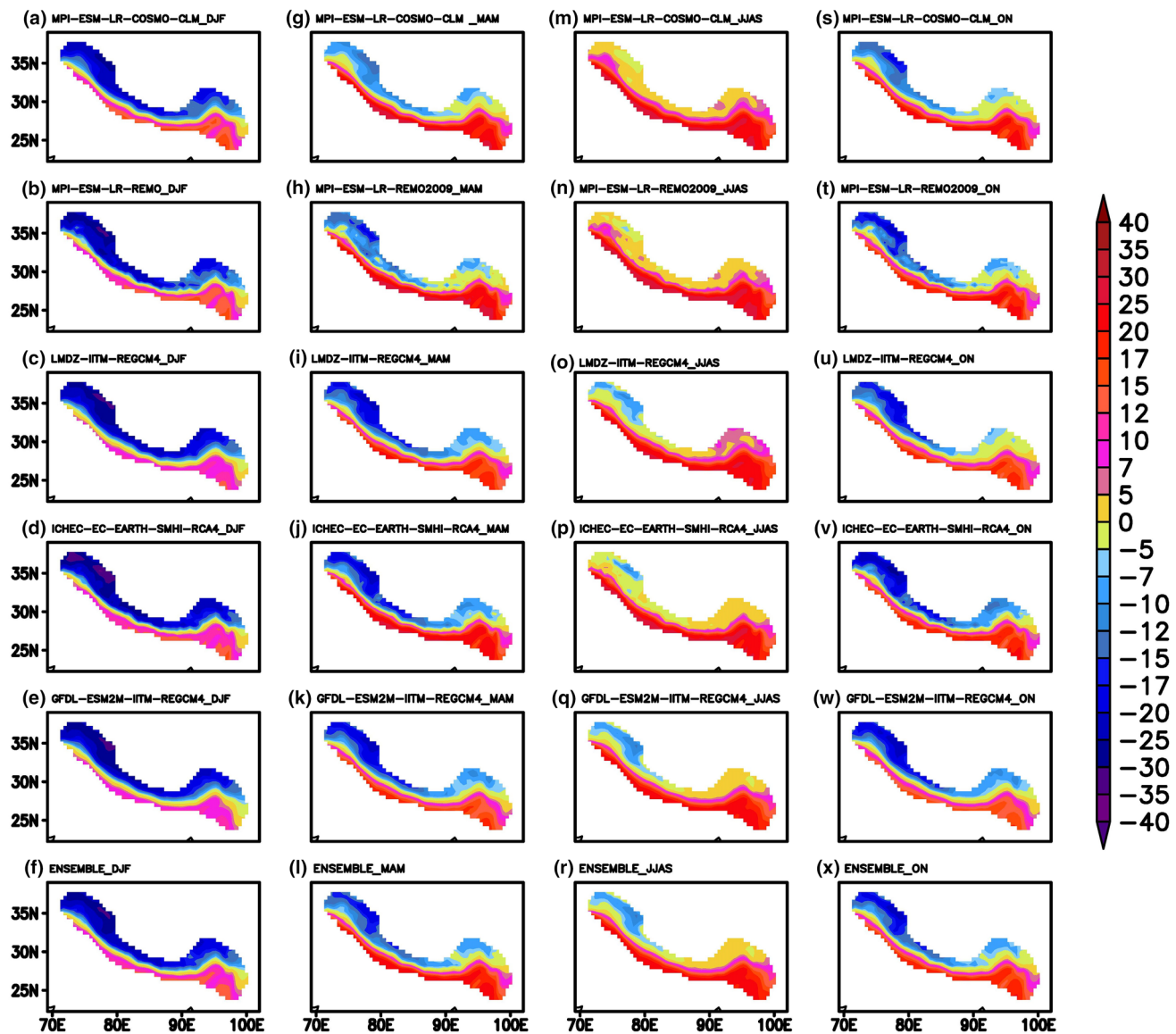


**Fig. 3** Seasonal mean temperature,  $T_{\text{mean}}$  ( $^{\circ}\text{C}$ ) climatology during 1970–2005 for the five CORDEX-SA experiments with their corresponding ENSEMBLE over the study area. *First column corresponds*

to winter (DJF); *second column corresponds to pre-monsoon (MAM), third column corresponds to monsoon (JJAS) and last column corresponds to post-monsoon (ON)*

temperature climatology is well reproduced by these models. The models also show the seasonal transition as the  $T_{\text{mean}}$  values vary across the study region ranging from  $-30$  to  $15^{\circ}\text{C}$  for DJF,  $-19$  to  $24^{\circ}\text{C}$  for MAM,  $-9$  to  $29^{\circ}\text{C}$  for JJAS and  $-21$  to  $20^{\circ}\text{C}$  for ON. Unlike Fig. 2, the model temperature during JJAS drops below  $0^{\circ}\text{C}$  at the higher reaches of the study region. One unique feature of the temperature regime of mountain microclimate is well captured by almost all the experiments in all the seasons irrespective of the model showing distinct temperature gradient between the foothill and the higher reaches of the Himalayas, driven mainly by the orographic forcing and the associated temperature lapse rate along the slope. Lu et al. (2004, 2006) suggested that landforms like mountains and

Tibetan plateau highly influences the seasonal temperature differences which are captured in the present set of regional climate models owing to its fine scale representation of topographic features. The north-western Himalayas remains at a cooler environment than the rest of the study region.

The errors in temperature represented by models have been quantified in terms of absolute bias of simulated  $T_{\text{mean}}$  climatology with corresponding APHROTEMP 0.5. As can be seen, Fig. 4, that all the models along with the ENSEMBLE show cold bias although its magnitude varies spatially and among the models but not so much in seasonal terms. Cold bias in simulated temperature with CRU dataset over the Hindu-Kush Himalaya region has been reported by Wiltshire (2014). Akhtar et al. (2009) reported similar cold

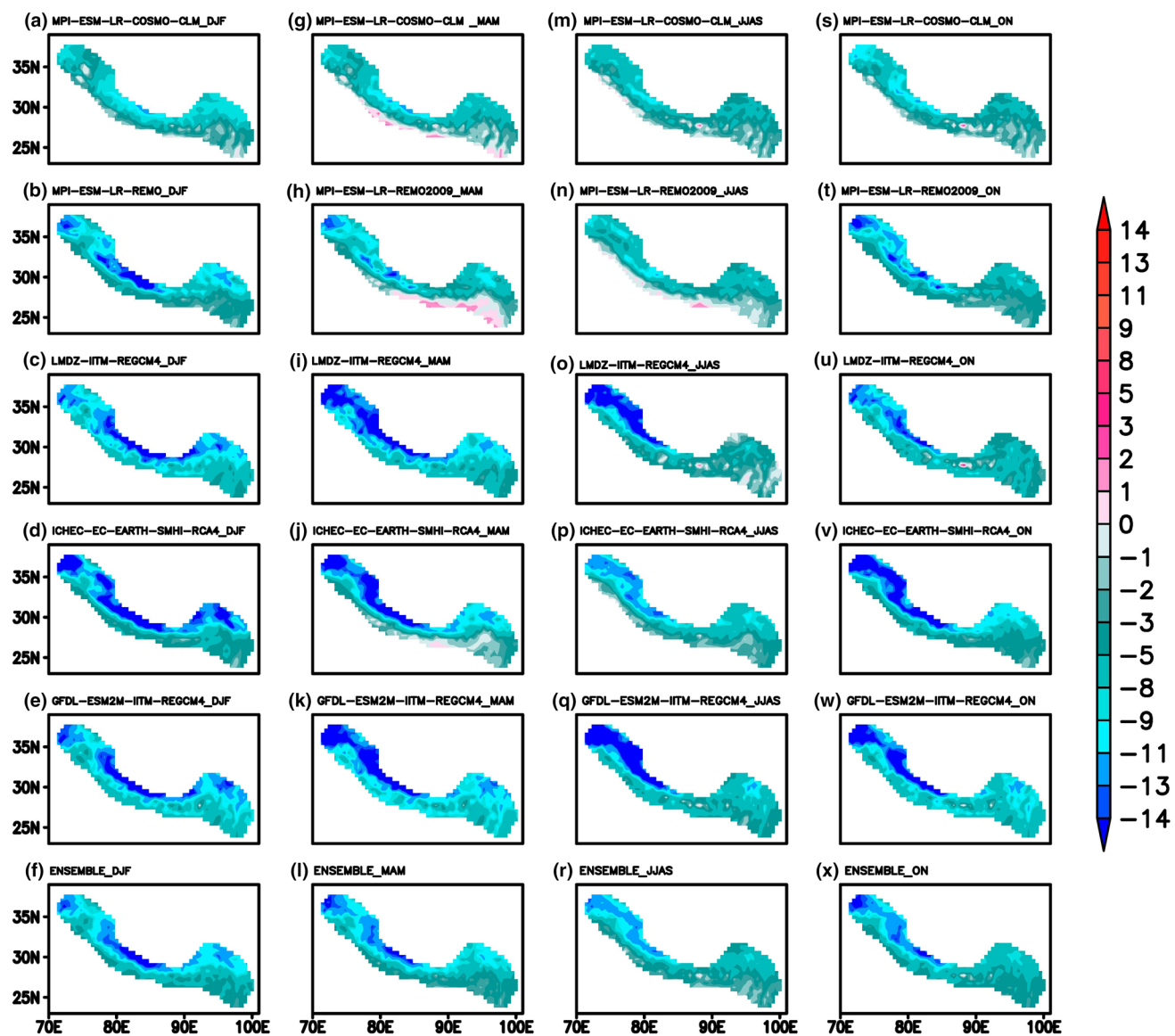


**Fig. 4** Same as Fig. 3, but for mean temperature,  $T_{\text{mean}}$  bias ( $^{\circ}\text{C}$ ) from APHROTEMP 0.5. First column corresponds to winter (DJF); second column corresponds to pre-monsoon (MAM), third column corresponds to monsoon (JJAS) and last column corresponds to post-monsoon (ON)

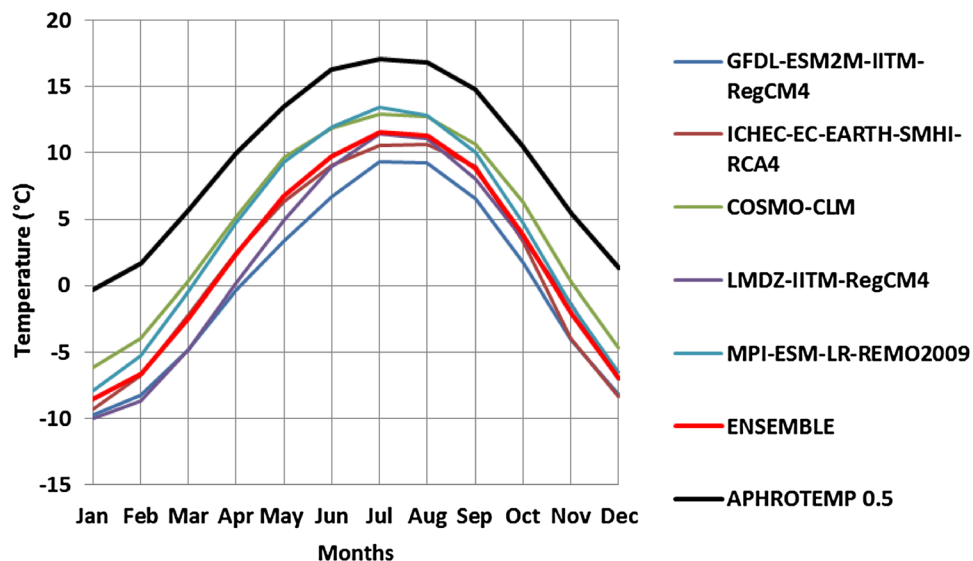
biases in temperature simulation in the Himalayan region from PRECIS regional model. He attributed the underestimation of temperature by the models to the bias present in the host GCMs. Furthermore, Giorgi et al. (2004), Solomon et al. (2008) and Haslinger et al. (2013) have shown cold bias in model simulations in mountainous regions as a common feature. Ghimire et al. (2015) in their study on precipitation simulation by similar set of CORDEX-SA models over the Himalayan region found an increasing wet bias in higher altitude. An overestimation of precipitation in the high altitudes can cause underestimation of temperature owing to the snow cover, moisture and evaporation feedbacks (Haslinger et al. 2013). In his study over three river basins of Himalaya (Indus, Ganga and Brahmaputra), Mishra (2015) has reported cold biases and large inter-model variability over all the three basins. We can see that there is a more prominent cold bias in the upper mountains than at the lower elevation region especially in the Central and Northwest Himalaya, as noted by Shi et al. (2011) in the northwest Tibetan plateau. This shows that the model performance varies spatially, there are regions where the models perform well and there also exist regions where the models show very large bias. The spatial variation of temperature bias also indicates toward topography dependent performance of models giving rise to region specific response to the surface forcings. Of all the five CORDEX-SA experiments, COSMO-CLM is better in capturing the temperature climatology as seen in its bias magnitude which seems to be smallest among all the models. Although all the models underestimate the actual temperature, along the foothills, COSMO-CLM (1st row, 2nd column) and REMO (2nd row, 2nd column) depicts warm bias for MAM season. Shi et al. (2011) also found greater cold bias in DJF compared to JJAS which is reflected as

a similar finding in our present study. Furthermore, the differences among model simulations could be due to difference in each model's configuration, parameterization physics or different parent GCMs used as a driving data for the RCMs. The inability of the model dynamics in accurately capturing the microphysical processes like albedo, cloud formation, latent heat etc. over the Himalayas could be responsible for these shortcomings. Figure 4 shows no considerable seasonal variation in of the distribution of bias across the region.

Annual cycle of simulated  $T_{\text{mean}}$  of the five CORDEX experiments, their ENSEMBLE and corresponding APHROTEMP 0.5 observation averaged over the study region during the study period is presented in Fig. 5. In general, the spread among the experiments is large throughout the year, however for July–August the experiments show similar distribution. Smallest value of simulated  $T_{\text{mean}}$  ( $-10^{\circ}\text{C}$ ) is shown in the month of January by LMDZ-IITM-RegCM4 and maximum simulated  $T_{\text{mean}}$  ( $13^{\circ}\text{C}$ ) is shown in the month of July by MPI-ESM-LR-REMO. Whereas, ENSEMBLE shows minimum  $T_{\text{mean}}$  ( $-8^{\circ}\text{C}/\text{year}$ ) in the month of January and maximum  $T_{\text{mean}}$  ( $11^{\circ}\text{C}/\text{year}$ ) in the month of July. Although all the experiments capture the  $T_{\text{mean}}$  distribution very efficiently, COSMO-CLM outperforms ENSEMBLE as the latter's performance is negatively affected by the other experiments. The figure depicts that all the models including ENSEMBLE underestimates the  $T_{\text{mean}}$  for every season.

Figure 6 shows the variation of observed  $T_{\text{mean}}$  with the elevation for four seasons. The  $T_{\text{mean}}$  values at each grid point within the study area averaged over the period of 36 years (1970–2005) is presented in the form of scatter plot with height. The number of gridpoints falling within each 1000 m of increasing altitude gives an idea of

**Fig. 5** Mean annual cycle of mean temperature,  $T_{\text{mean}}$  ( $^{\circ}\text{C}$ ) over the period of 1970–2005 averaged over study region for five CORDEX-SA experiments, ENSEMBLE and corresponding APHROTEMP 0.5. Nomenclature corresponds to respective CORDEX-SA experiments



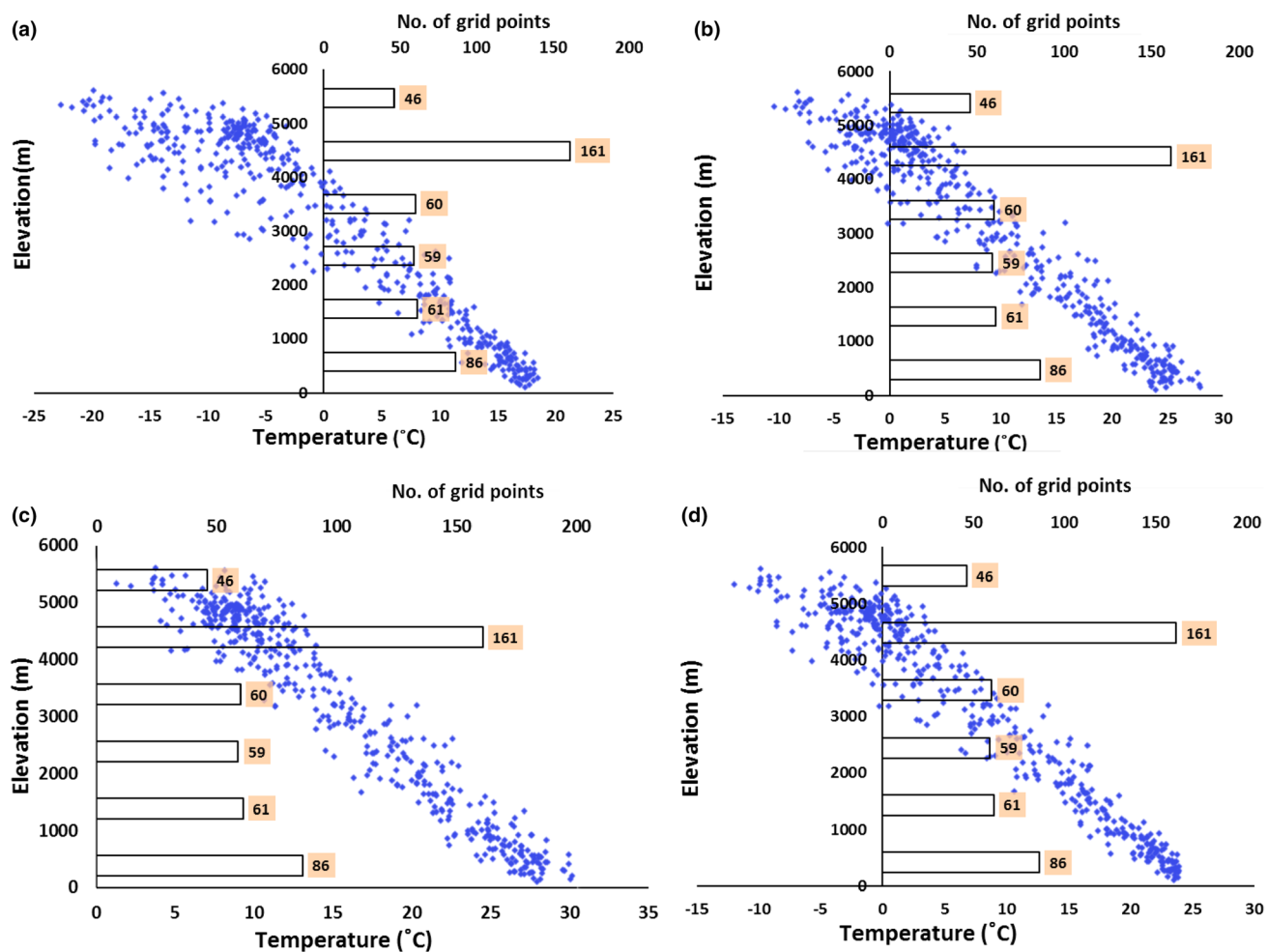


**Fig. 6** Variation of observed mean temperature,  $T_{\text{mean}}$  ( $^{\circ}\text{C}$ ) with elevation (m) for different seasons—**a** DJF, **b** MAM, **c** JJAS, **d** ON for APHROTEMP 0.5

topographic distribution in the study region. In Fig. 6, a linear relationship between elevation and temperature distribution corresponding to our understanding of the slope environmental lapse rate is seen. Compared to lower elevation points there is larger spread in the temperature in the higher elevation points which suggests higher spatial variability of the  $T_{\text{mean}}$  values in this region. This is possibly because of a differential climatic response of surface forcings to sharp orographic changes and latitudinal differences at the higher elevation region. According to Lu et al. (2010) high altitude area (below 5000 m) of the Himalayas and Tibetan plateau does not respond to global warming as effectively as the low-altitude regions. It is mainly caused by the high albedo, large thermal capacity of snow/ice cover in the higher elevation, since snow is an active agent of climatic variability (Walsh et al. 1985). Therefore the sharp topographic changes at high altitudes dominate the induced temperature variability more than the large scale warming tends to reduce the variability. Another reason for

the reduced variability at lower elevations could be related to the heat island effect owing to higher trends of urbanization there. Also, according to Kalnay and Cai (2003), the land use change and urbanisation impacts on the surface warming cannot be ignored.

A similar pattern in variation of  $T_{\text{mean}}$  with elevation is observed in all the experiments and their ENSEMBLE (Fig. 7). The models are able to capture the lapse rate based decrease in temperature with elevation. COSMO-CLM, REMO and ICHEC also captures the seasonal variation in altitudinal distribution of temperature. Further, we notice that the spread of simulated  $T_{\text{mean}}$  increases with altitude which is discussed earlier in observation also. Local climatic effects damp out the temperature anomalies at lower altitudes which results in smaller variability over such regions (Beniston and Rebetez 1996). We also see a seasonal dependency of spatial variability from middle to higher altitudes as spread seems to be least during the monsoon but most during the winter. It is probably due to

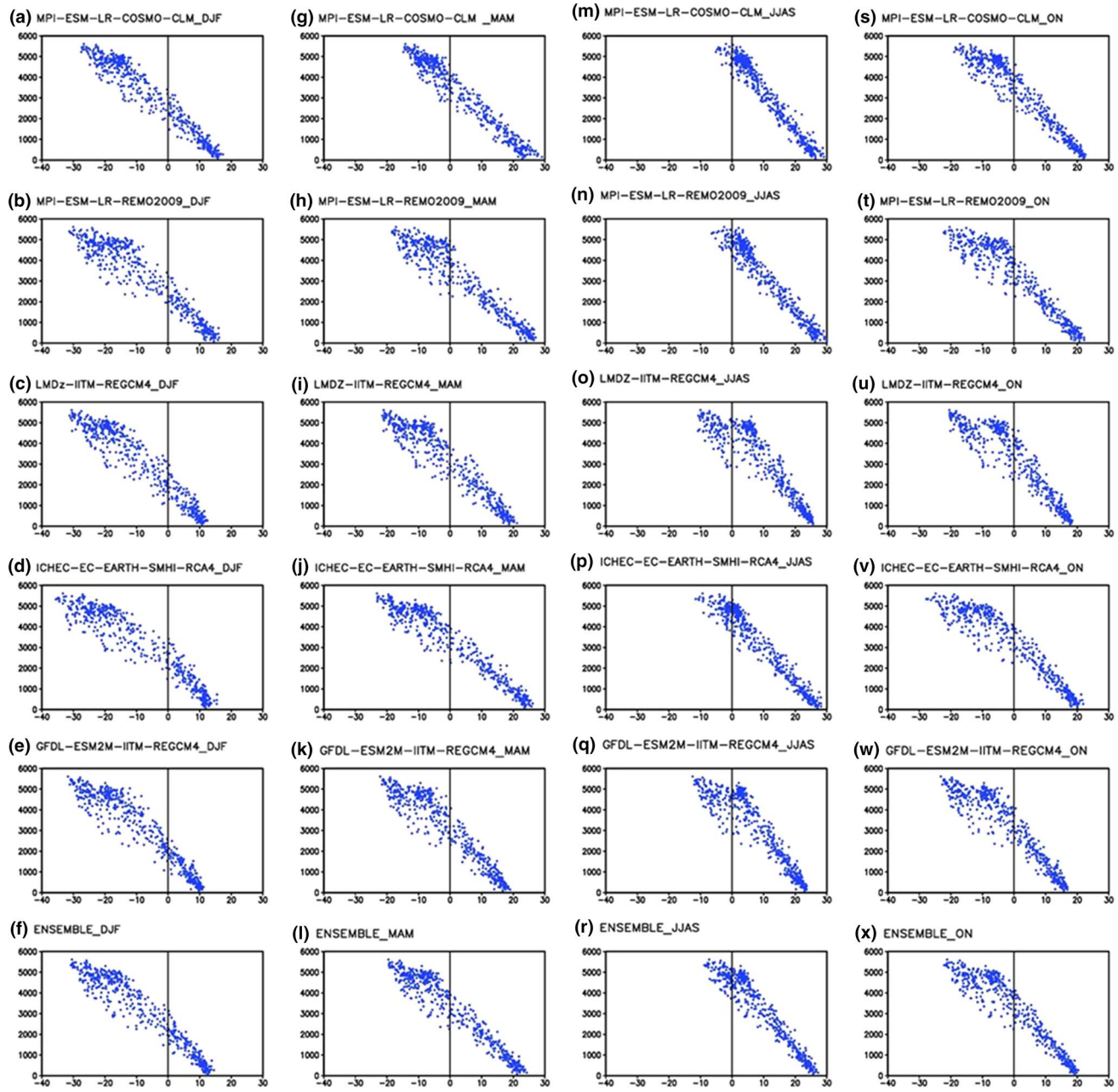


**Fig. 7** Variation of mean temperature,  $T_{\text{mean}}$  ( $^{\circ}\text{C}$ ) with elevation (m) for different seasons for five CORDEX-SA experiments and their corresponding ENSEMBLE. *First column* corresponds to winter (DJF);

*second column* corresponds to pre-monsoon (MAM), *third column* corresponds to monsoon (JJAS) and *last column* corresponds to post-monsoon (ON)

the dominant role of moisture-temperature interplay which regulates the spatial variability of temperature in the form of latent heat storage in the model environment and reduces the variability during the monsoon season.

Figure 8 shows consistent pattern in the variation of model  $T_{\text{mean}}$  biases (from APHROTEMP) with altitude to look for any elevation dependent shortcomings in the model. Each experiment for all the four seasons shows cold bias as found in the earlier discussions on climatology.

Underestimation of temperature is more prominent at higher elevations which means that the model environment is colder than the real environment at higher elevations. In Fig. 8, there is a clear intensification of cold bias with height. Haslinger et al. (2013) also found a similar relation between model skill and altitude over the Alpine region. Ghimire et al. (2015) in their study on precipitation simulation by a similar set of CORDEX-SA models over the Himalayan region found an increasing wet bias at

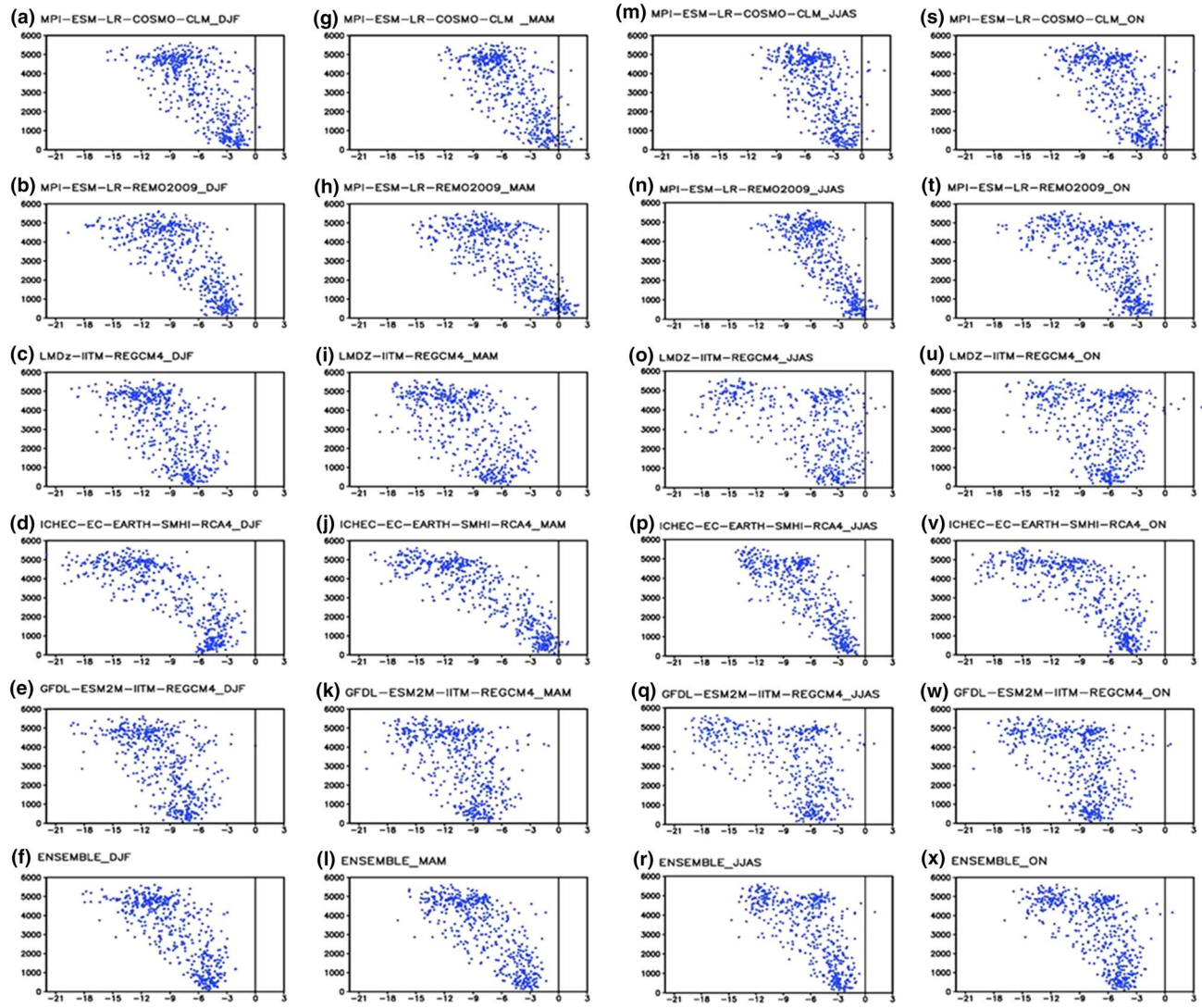


**Fig. 8** Variation of seasonal mean temperature,  $T_{\text{mean}}$  bias ( $^{\circ}\text{C}$ ) with elevation (m) for the five CORDEX-SA experiments and their corresponding ENSEMBLE from APHROTEMP 0.5. First column corresponds to winter (DJF); second column corresponds to pre-monsoon (MAM), third column corresponds to monsoon (JJAS) and last column corresponds to post-monsoon (ON)

responds to winter (DJF); second column corresponds to pre-monsoon (MAM), third column corresponds to monsoon (JJAS) and last column corresponds to post-monsoon (ON)

higher altitudes. The relationship between altitudinal variation of temperature bias and that of precipitation bias might be resulting from an overestimation of precipitation in the high altitudes. Wet bias can cause underestimation of temperature owing to the snow cover, moisture and evaporation feedbacks (Haslinger et al. 2013). The cold bias can further be attributed to model environmental lapse rate being greater than that in the realistic environment. However, at lower elevation regions COSMO-CLM and REMO shows pre-monsoon (MAM) warm bias at some of the gridpoints (Fig. 8g, h). It is seen that the (cold) bias gradually increases with elevation though at the higher altitudes, there seems to be a large spread in the biases owing to the higher degree of spatial variability in the temperature at

such elevations which are discussed before. The inclusion of topography in RCM could also result in model environment becoming highly variable in space. The effective forcing of local topography and thereby the complexity in the simulation leads to high variability in the model and hence, model performance also varies.

Figure 9 presents the yearly variability of  $T_{\text{mean}}$  for different observations in terms of standard deviation of 36 years' seasonal mean temperature values at each grid point in the study area. There are slight differences among the various observations as the variability does not change much across the space. It also reveals a common pattern in the representation of yearly variability of  $T_{\text{mean}}$  values for each observation and for every season. Least deviation in

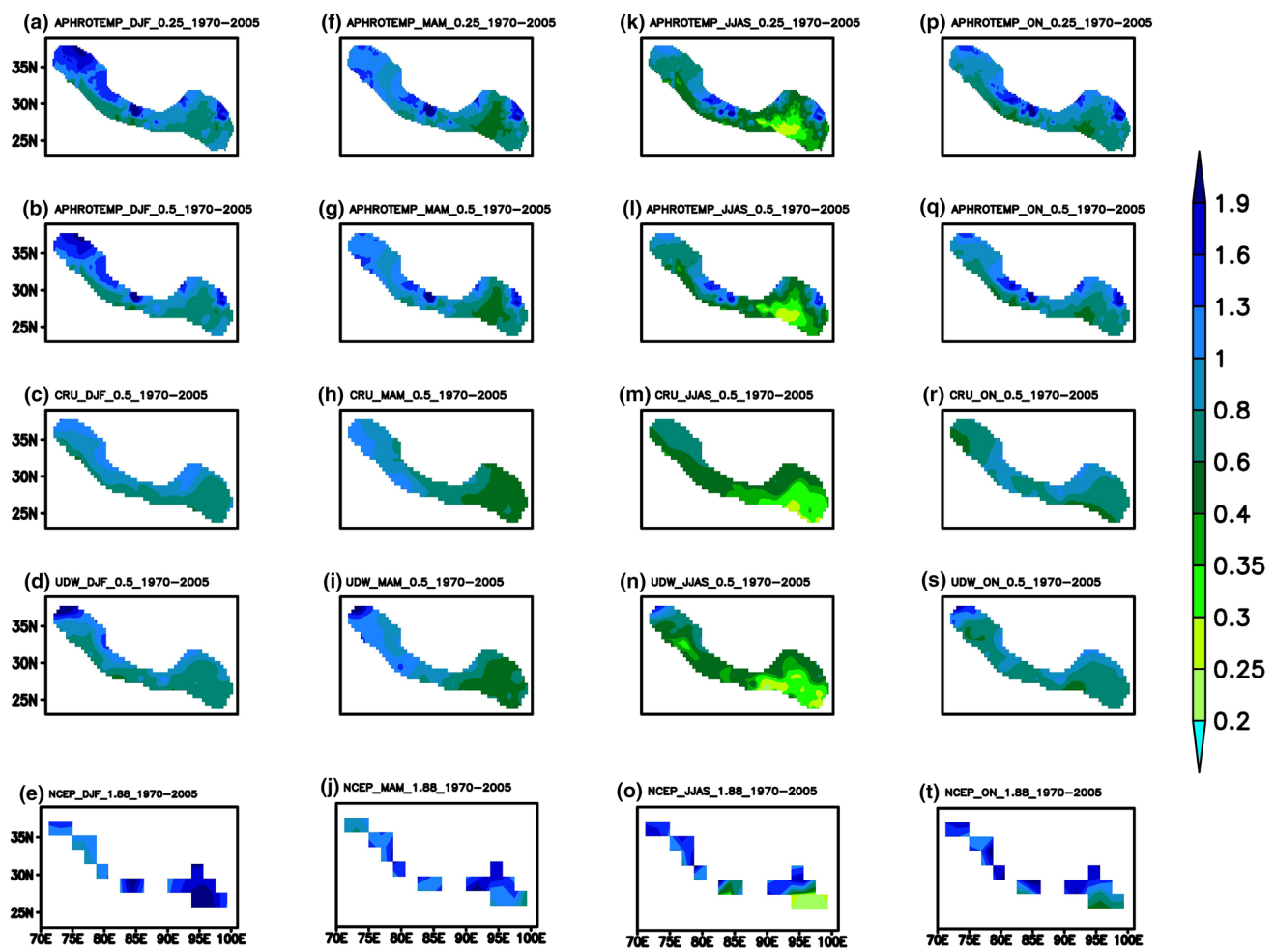


**Fig. 9** Yearly variability in seasonal mean temperature,  $T_{\text{mean}}$  values (as standard deviation,  $^{\circ}\text{C}$ ) for different observations during 1970–2005. First column corresponds to winter (DIF); second column cor-

responds to pre-monsoon (MAM), third column corresponds to monsoon (JJAS) and last column corresponds to post-monsoon (ON)

the  $T_{\text{mean}}$  values is observed in the JJAS (monsoon) season in all the observations (Fig. 9k–o). This implies that the JJAS year-wise seasonal mean temperature does not deviate much from the mean climate at each grid point. This may indicate that the monsoon season due to the dominant role of moisture and large solar flux is less sensitive to climatic scale temporal variability. APHROTEMP 0.5 shows highest variability in the  $T_{\text{mean}}$  values during DJF which is consistent with findings of Stahl et al. (2006) and Daly (2006). As discussed in the previous analysis, the variability is greater over the higher reaches of the western Himalayas which possibly points towards a higher sensitivity of this region to the natural climatic changes.

The model simulated yearly variability in the  $T_{\text{mean}}$  values is presented in Fig. 10. The models show higher variability in space when compared with the corresponding observation APHROTEMP 0.5. However, the seasonal transition of observed variability is captured by the models

as we see smallest variability during JJAS and highest during DJF (Stahl et al. 2006; Daly 2006). From this analysis we find that the models in general are able to capture the seasonal changes in observed variability with slight overestimations at higher altitudes.

Several studies viz. Diaz and Bradley (1997), Benniston (2003), Rebetez (2004) and Jomelli et al. (2004) have shown a rising temperature trend in mountainous regions across the world. In Fig. 11a–t the spatial distribution of  $T_{\text{mean}}$  trend ( $^{\circ}\text{C}/\text{year}$ ) of five different observations are shown. A mixed spatial pattern of warming–cooling zones are seen in the study region except for CRU which shows consistent warming throughout the region. Remarkably, a cooling trend is observed in a distinct patch in eastern Himalayas and in some patches of western Himalayas for almost all seasons. This indicates that these regions may be defying the global scale warming phenomena which is similar to findings by Yadav et al. (2004) and Hewitt

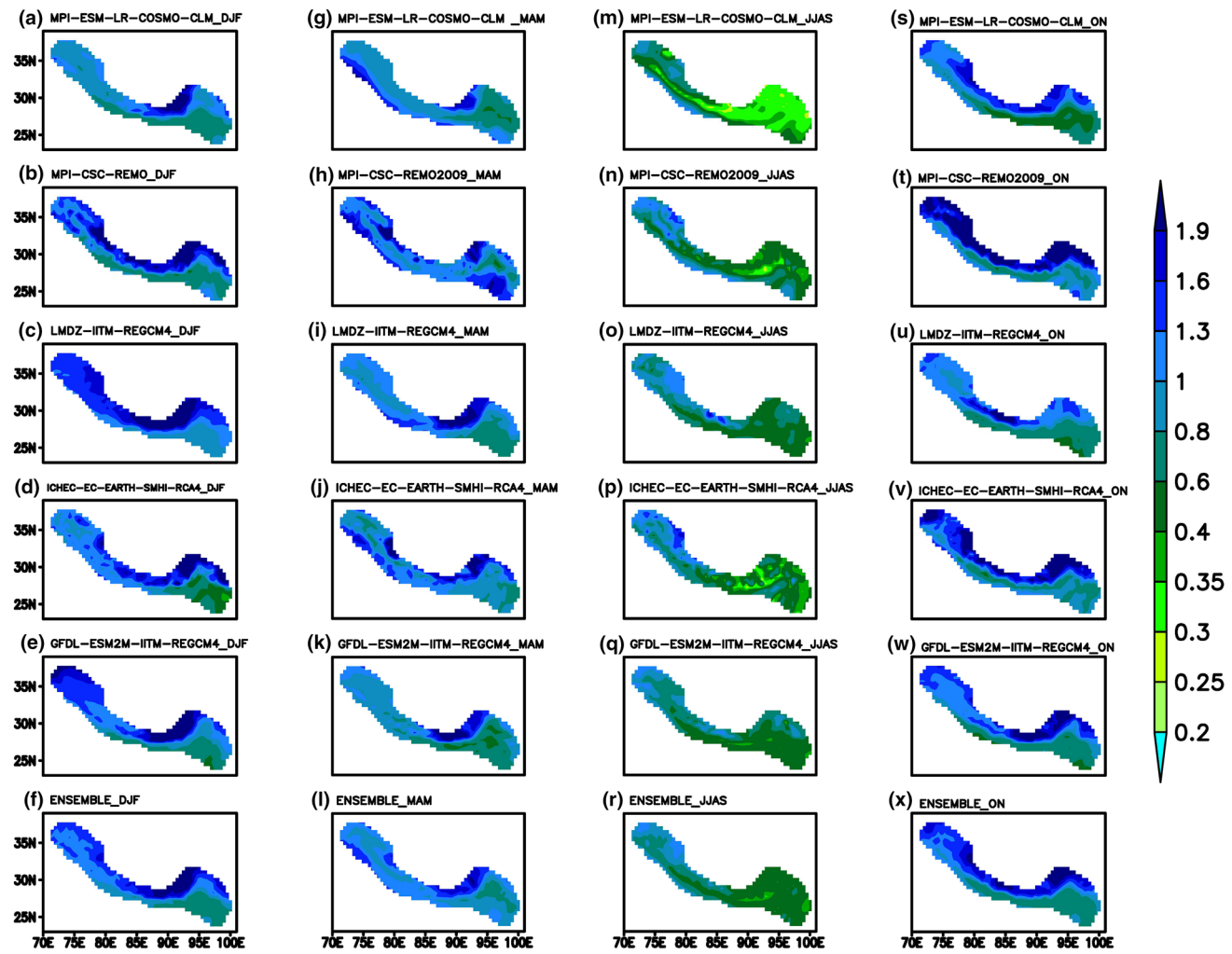


**Fig. 10** Yearly variability in seasonal mean temperature,  $T_{\text{mean}}$  values (as standard deviation,  $^{\circ}\text{C}$ ) for five CORDEX-SA experiments and their corresponding ENSEMBLE during 1970–2005. *First column*

corresponds to winter (DJF); *second column* corresponds to pre-monsoon (MAM), *third column* corresponds to monsoon (JJAS) and *last column* corresponds to post-monsoon (ON)

(2005). Such anomalous cooling could be due to changes in local land-use patterns that induce negative forcings with respect to surface irradiative properties. For APHROTEMP 0.5 this cooling trend is around  $0.1^{\circ}\text{C}/\text{year}$  although APHROTEMP 0.5 do not show any seasonal variation in the  $T_{\text{mean}}$  values. Also, in NCEP the pre-monsoon cooling is quite evident (a phenomena described by Yadav et al. 2004) which is not so in the case of other observations. In Fig. 11c, d, the winter warming is well captured by CRU and UDW, a phenomena also observed by others over the Himalayas (Bhutiyani et al. 2007; You et al. 2010; Rajbandari et al. 2015). Greater warming in DJF compared to JJAS over the Tibetan plateau and Nepal Himalaya signalling higher sensitivity of winter season towards global warming have also been reported by Zhou et al. (2003), He et al. (2005), Li et al. (2005), Yang et al. (2011), Yang and Achim (2006), Zhang et al. (2006), Rangwala et al. (2009),

Shrestha and Aryal (2011) and Shi et al. (2011). Enhanced winter warming is attributed to an amplified water vapour feedback at high altitudes during winter season (Rangwala 2013). Increase in surface moisture during winter produces relatively large increase in downward long-wave radiation when the surface moisture is  $2.5 \text{ g/kg}$  or less, which is usually the condition during winter months as the atmosphere is comparatively drier especially at higher altitudes (Rangwala et al. 2009).

We examine the simulated trends of  $T_{\text{mean}}$  in comparison with that of APHROTEMP0.5 in Fig. 12. Spatial distribution of  $T_{\text{mean}}$  trend for five CORDEX experiments and their ENSEMBLE for different seasons are presented here. A striking feature from this figure comes out that trend signal differs between the models and the observation and for every season. The models show stronger positive trend than the observation which means an intensified warming in

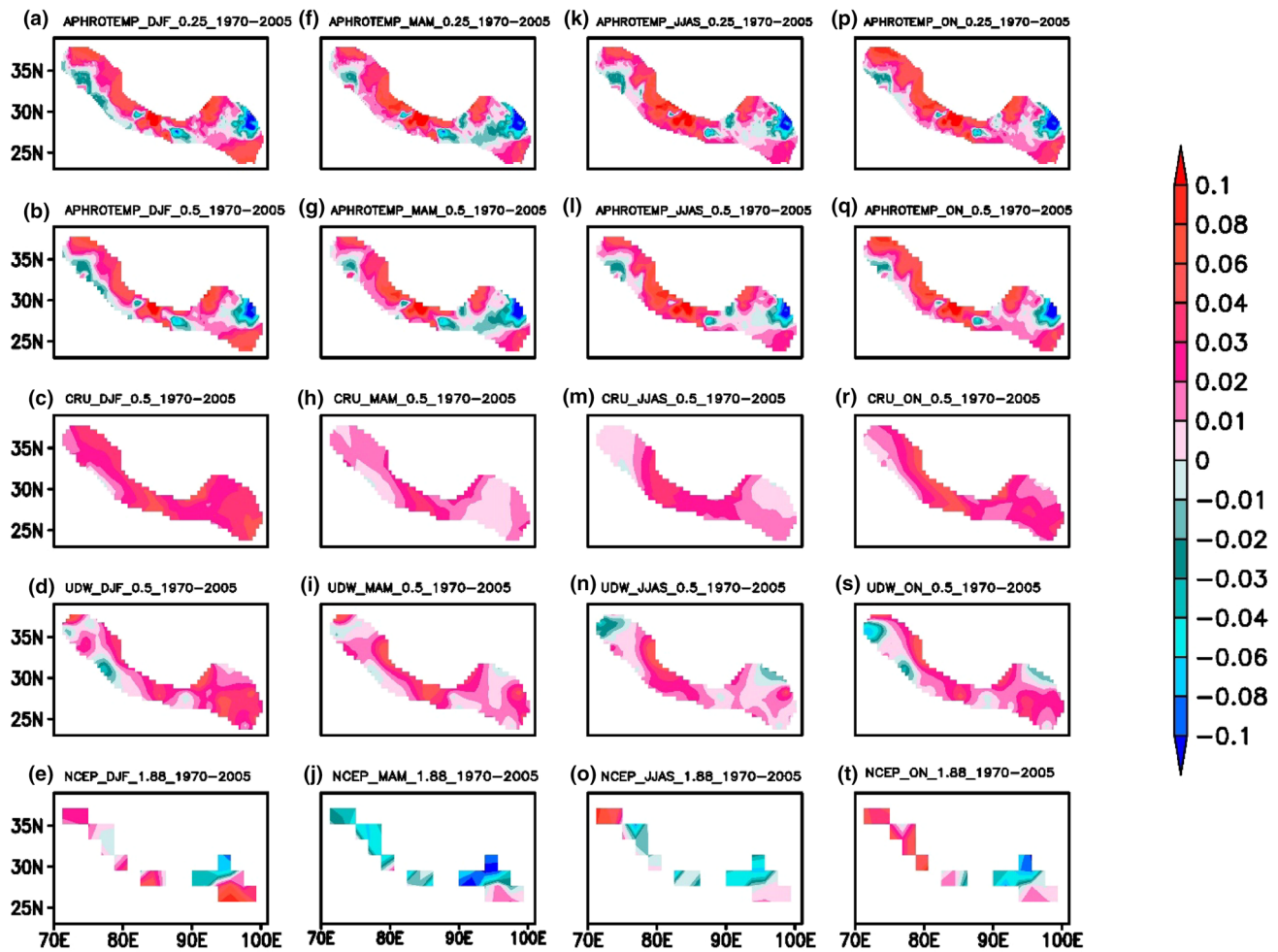


**Fig. 11** Trend of seasonal mean temperature,  $T_{\text{mean}}$  ( $^{\circ}\text{C}/\text{year}$ ) for different observations during 1970–2005. First column corresponds to winter (DJF); second column corresponds to pre-monsoon (MAM),

third column corresponds to monsoon (JJAS) and last column corresponds to post-monsoon (ON)

the model environment. This is despite the cold bias in the models as observed in Figs. 4 and 8. If we consider a single experiment and compare the results for different seasons e.g. for COSMO-CLM, as shown in the first row that the models show least rate of warming during the JJAS season over the entire Himalayan region, whereas highest warming magnitude is seen during DJF season (Rangwala and Miller 2012). This was also seen earlier in case of observations and reasons were discussed at the end. LMDz-IITM-REGCM4 shows very high rate of winter warming across the entire study region (Fig. 12c). Except for REMO (2nd row, Fig. 12) rest of the models tends to show warming in the high elevation region of the northwest Himalayas.

Despite extensive efforts to study the elevation dependent warming in mountainous regions carried out by different researchers (Wang et al. 2014; Rangwala and Miller 2012; Lu et al. 2010; Liu et al. 2009; Pepin and Lundquist 2008; Pepin and Seidel 2005; Yan and Liu 2014; Beniston

2003; Beniston et al. 1997; Diaz and Bradley 1997) our understanding of the effects of elevation on warming pattern is limited and uncertain. The study of climate change in mountainous region is a complex one. Inadequacies in observation and limited representation of the details of mountain physiography and climate system in models (Rangwala and Miller 2012), studies confined to specific region (Beniston et al. 1997; Liu et al. 2009; Ohmura 2012; Wang et al. 2013), incompatible data (Ohmura 2012), different methodologies (Liu et al. 2009) contribute to the issues. As observed by Seidel and Free (2003) there is a huge difference in the nature and representation of climatic variability of high mountainous region from that of the low elevation region. Further research studies have also been carried out by Liu and Chen (2000), Stewart (2009) and Forstythe et al. (2014) to widen the understanding of the dynamics of climate in the mountain regions. Based on the surface observations by Pepin and Seidel (2005); Pepin

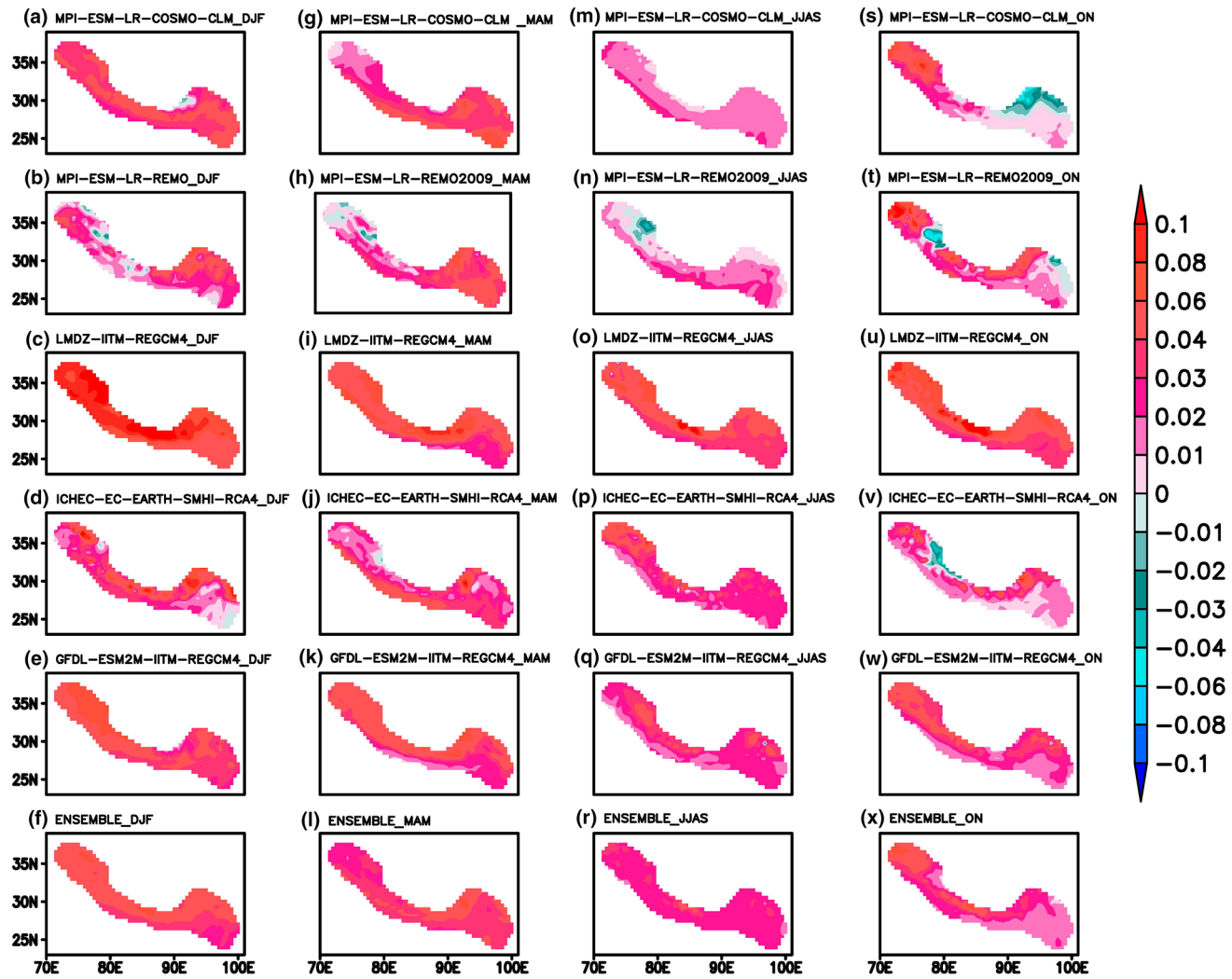


**Fig. 12** Trend of seasonal mean temperature,  $T_{\text{mean}}$  ( $^{\circ}\text{C}/\text{year}$ ) for five CORDEX-SA experiments and their ENSEMBLE during 1970–2005. First column corresponds to winter (DJF); second column corre-

sponds to pre-monsoon (MAM), third column corresponds to monsoon (JJAS) and last column corresponds to post-monsoon (ON)

and Lundquist (2008), no significant correlation was found between elevation and rate of warming on the global scale. Pepin and Lundquist (2008) reasoned that the observed pattern of change in temperature was controlled by snow-ice feedback. They also asserted that consistent warming rate in the mountain summit depends on the factors like topography and exposure that affects the warming conditions while the distinguished valleys unlike higher elevations show highly variable warming rates in time. Similar studies by Diaz and Bradley (1997) shows that the trends in maximum temperature were less consistent with elevation, showing the maximum warming at 500–1000 m.

Model studies by Snyder et al. (2002), Chen et al. (2003) and Kotlarski et al. (2012) suggests that climate change might depend on elevation, mainly owing to the increase in the  $\text{CO}_2$  in the atmosphere. A clear elevation

dependent warming was observed by Yan and Liu (2014) over the Tibetan Plateau over the last 50 years and also they observed a higher rate of warming and greater elevation dependency in the recent decades. Yan and Liu (2014) also reported the positive trend of warming with elevation for the mean minimum temperature on annual basis and also for mean annual temperature in autumn and winter seasons. There was no consistent increase in the rate of warming with elevation observed for mean maximum temperature. Similarly, several studies suggest the linear relationship between the elevation and higher rate of warming with elevation (Beniston and Rebetez 1996; Diaz and Bradley 1997; Liu and Hou 1998; Liu and Chen 2000; Liu et al. 2009; Wang et al. 2013). However, some studies also suggests otherwise (Vuille and Bradley 2000; Pepin and Losleben 2002; Lu et al. 2010). You et al. (2010) reasoned that

factors like topography and differences in the model physics contributed towards the differences of trend observed.

Keeping in view the previous works carried out in various mountainous regions across the globe, we have tried here to understand the dependence of warming on elevation in the Himalayan region based on observational data as well as in model environment. For observation, Fig. 13 shows a similar picture of positive (yearly) trend throughout the entire altitudinal stretch and across all the seasons with not much difference in the overall pattern. Table 2 confirms this finding where we have a positive average trend in all elevation ranges except between 3500 and 4000 m where a decreasing trend of temperature is noticed in all seasons. For this range we also found that the trend decreases with height (negative correlation) for all seasons whereas above 4000 m the trend increases with height clearly indicating the transitional point of elevation dependent warming. Furthermore, we see strongest positive correlation of around 0.3 between trend and height in lowermost elevations (0–500 m) and also between 3000 and 3500 m in all seasons. There also exists a spatial variability in trend values (see Table 2) which seems to be more in middle elevation

ranges (3000–4500 m) compared to the extreme ones. Focusing specifically within different ranges of elevations, it is noticed that, Fig. 13, gridpoints at the lower elevations (below 1000 m) during DJF show a warming rate as high as 0.05 °C/year whereas during JJAS the same is limited upto only about 0.025 °C/year—an indication of seasonality in trends which supports the winter warming phenomena. Nevertheless, no such pattern is observed at the higher elevations which is similar to findings by Pepin and Seidel (2005) and You et al. (2008). Except during DJF, for the grid points lying above 4000 m the rate of warming on an average seems to be higher than those below 1000 m. Using the ice core method Kang et al. (2007) and Tian et al. (2006) have also reported a warming trend in the regions at high elevations around 6000 m. Besides, warming trend which is observed at most of the gridpoints, a cooling trend is also noticed but limited for few gridpoints at both high and lower elevation zones and magnitude of which does not vary much across the seasons. In Fig. 14, it is seen that the distribution of temperature trend with elevation varies widely across the models in all seasons. This implies towards uncertainty in simulated temperature over

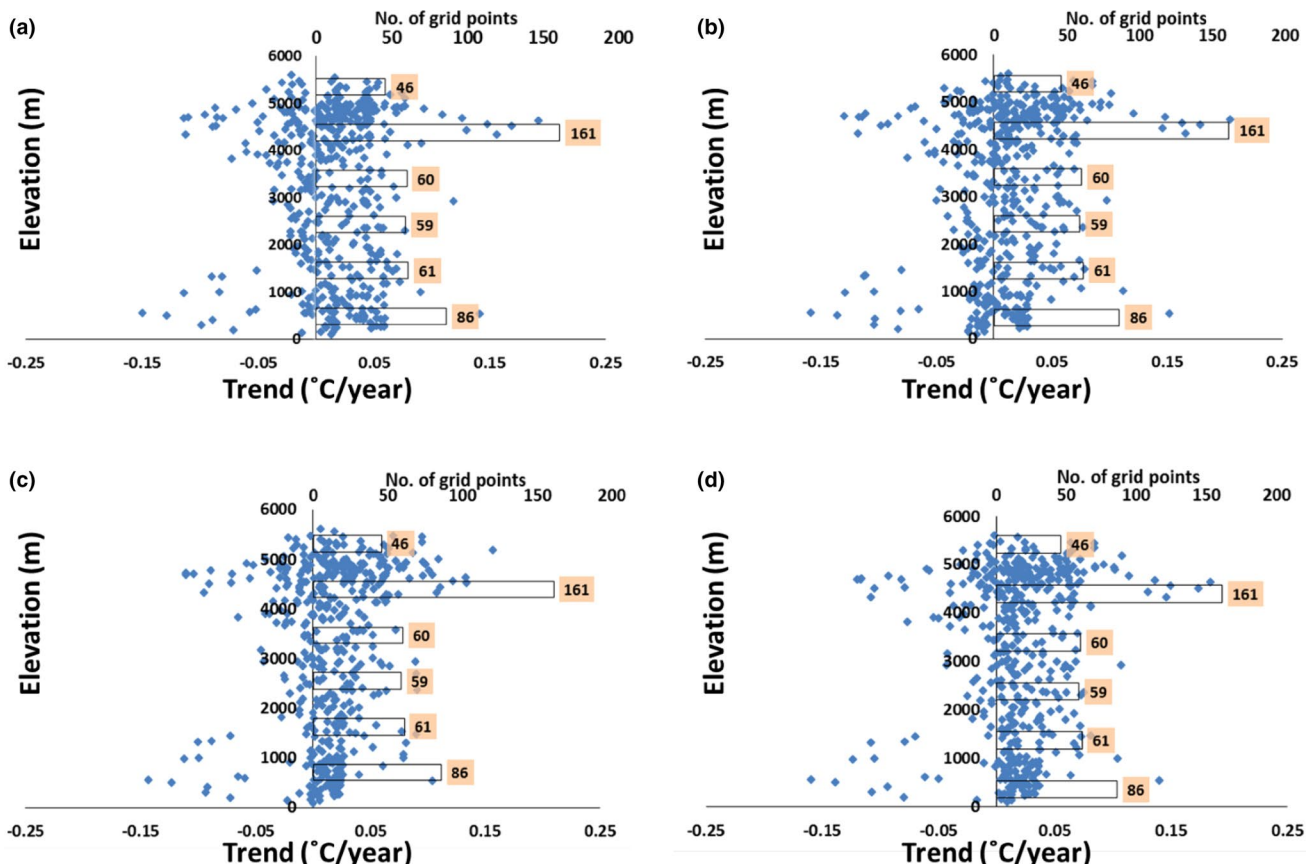


**Fig. 13** Variation in trend ( $^{\circ}\text{C}/\text{year}$ ) with elevation (m) of mean temperature,  $T_{\text{mean}}$  for APHROTEMP 0.5 for different seasons—**a** DJF, **b** MAM, **c** JJAS and **d** ON

**Table 2** Average trend ( $^{\circ}\text{C}/\text{year}$ ) of seasonal mean temperature over the grid points within each 500 m elevation range along with corresponding standard deviation (representing spatial variability of trend) in brackets and correlation of trend with elevation (in brackets its

significance as p value) for observation—APHROTEMP 0.5 (here, APH) and the ensemble mean (here, ENS) of all the five CORDEX-SA experiments as described in Table 1 during four seasons—DJF, MAM, JJAS and ON

Elevation range in meters (mean elevation) (No. of grid points)	DJF				MAM			
	Trend, $^{\circ}\text{C}/\text{year}$ (standard deviation)		Correlation (significance)		Trend, $^{\circ}\text{C}/\text{year}$ (standard deviation)		Correlation (significance)	
	APH	ENS	APH	ENS	APH	ENS	APH	ENS
0–500 (325.56) (34)	0.02 (0.02)	0.03 (0)	0.25 (0.15)	-0.07 (0.71)	0 (0.02)	0.04 (0)	0.38 (0.03)	0.06 (0.75)
500–1000 (739.3) (52)	0.01 (0.02)	0.03 (0)	0.05 (0.75)	0.05 (0.74)	0 (0.02)	0.04 (0)	0.07 (0.6)	0.11 (0.45)
1000–1500 (1246.98) (30)	0.01 (0.03)	0.04 (0.01)	0.12 (0.54)	0.11 (0.58)	0.01 (0.02)	0.04 (0.01)	0.3 (0.1)	0.4 (0.03)
1500–2000 (1754.07) (31)	0.01 (0.03)	0.04 (0.01)	-0.29 (0.12)	0.37 (0.04)	0.01 (0.03)	0.04 (0.01)	-0.21 (0.26)	0.13 (0.49)
2000–2500 (2265.48) (31)	0 (0.03)	0.04 (0.01)	-0.1 (0.6)	0.28 (0.13)	0 (0.04)	0.04 (0.01)	0 (0.99)	-0.11 (0.55)
2500–3000 (2793.62) (28)	0 (0.03)	0.04 (0.01)	0.22 (0.27)	-0.12 (0.53)	0 (0.03)	0.03 (0.01)	0.15 (0.45)	-0.13 (0.5)
3000–3500 (3248.59) (28)	0.01 (0.03)	0.05 (0.01)	0.26 (0.18)	0.15 (0.45)	0.01 (0.03)	0.03 (0.01)	0.27 (0.16)	0.3 (0.12)
3500–4000 (3774.05) (32)	-0.01 (0.05)	0.05 (0.01)	-0.17 (0.35)	0.09 (0.01)	-0.01 (0.06)	0.03 (0.01)	-0.2 (0.26)	0.5 (0)
4000–4500 (4253.13) (51)	0 (0.05)	0.05 (0)	0.1 (0.48)	-0.19 (0.18)	0 (0.06)	0.03 (0)	0.1 (0.5)	-0.07 (0.61)
4500–5000 (4763.64) (110)	0.03 (0.03)	0.05 (0.01)	0.18 (0.06)	-0.01 (0.88)	0.03 (0.04)	0.04 (0.01)	0.19 (0.04)	0.08 (0.4)
5000–5500 (5209.63) (44)	0.04 (0.02)	0.05 (0.01)	0.05 (0.73)	-0.22 (0.16)	0.04 (0.03)	0.04 (0.01)	0.1 (0.51)	-0.56 (0)
5500–6000 (5585.69) (2)	0.03 (0)	0.05 (0)			0.04 (0)	0.03 (0)		
Elevation range in meters (mean elevation) (No. of grid points)	JJAS				ON			
	Trend, $^{\circ}\text{C}/\text{year}$ (standard deviation)		Correlation (significance)		Trend, $^{\circ}\text{C}/\text{year}$ (standard deviation)		Correlation (significance)	
	APH	ENS	APH	ENS	APH	ENS	APH	ENS
0–500 (325.56) (34)	0.01 (0.01)	0.02 (0)	0.27 (0.12)	0.01 (0.95)	0.02 (0.01)	0.02 (0)	0.35 (0.04)	0.01 (0.94)
500–1000 (739.3) (52)	0.01 (0.02)	0.02 (0)	-0.01 (0.93)	-0.02 (0.88)	0.01 (0.01)	0.02 (0)	-0.09 (0.53)	0.05 (0.73)
1000–1500 (1246.98) (30)	0.01 (0.02)	0.02 (0)	0.21 (0.28)	-0.06 (0.77)	0.02 (0.02)	0.02 (0)	0.13 (0.48)	0.21 (0.27)
1500–2000 (1754.07) (31)	0.01 (0.03)	0.02 (0)	-0.27 (0.14)	-0.01 (0.97)	0.01 (0.03)	0.02 (0)	-0.18 (0.32)	0.26 (0.16)
2000–2500 (2265.48) (31)	0.01 (0.04)	0.02 (0)	-0.07 (0.72)	0.24 (0.19)	0.01 (0.04)	0.02 (0)	-0.09 (0.62)	0.24 (0.18)
2500–3000 (2793.62) (28)	0 (0.03)	0.02 (0)	0.08 (0.67)	0.05 (0.8)	0 (0.03)	0.03 (0)	0.19 (0.33)	0 (1)
3000–3500 (3248.59) (28)	0.01 (0.04)	0.03 (0)	0.28 (0.15)	-0.12 (0.54)	0.01 (0.04)	0.03 (0)	0.27 (0.16)	-0.1 (0.61)
3500–4000 (3774.05) (32)	-0.01 (0.06)	0.03 (0)	-0.19 (0.29)	0.09 (0.61)	-0.01 (0.06)	0.03 (0)	-0.19 (0.29)	-0.33 (0.06)
4000–4500 (4253.13) (51)	0.01 (0.05)	0.03 (0)	0.12 (0.41)	-0.09 (0.54)	0.02 (0.06)	0.04 (0)	0.09 (0.53)	-0.05 (0.71)
4500–5000 (4763.64) (110)	0.03 (0.03)	0.03 (0.01)	0.2 (0.03)	0.02 (0.84)	0.04 (0.03)	0.03 (0.01)	0.19 (0.05)	-0.01 (0.91)
5000–5500 (5209.63) (44)	0.04 (0.03)	0.03 (0.01)	0.23 (0.13)	0.07 (0.66)	0.05 (0.03)	0.03 (0.01)	0.16 (0.3)	-0.38 (0.01)
5500–6000 (5585.69) (2)	0.03 (0)	0.03 (0)			0.04 (0.01)	0.02 (0)		

To see the results for individual experiments refer to supplementary tables – S1, S2, S3, S4 and S5

the Himalayan region. Also unlike observation, the models and their ENSEMBLE show a clearer response to seasonal changes in terms of variable warming rates and its distribution with height (as correlation) (see Table 2 and supplementary tables). One thing which is inferred from the present study is that the high elevation grid points behave differently in response to the warming in the model environment. This could be due to differential sensitivity of surface warming to changes in climatic drivers at different elevations. As seen in the observation, the trends in the ENSEMBLE during DJF and ON increases with elevation suggesting that the seasonal dependency of elevation

dependent warming is captured to some extent in the models. Further, Fig. 15 presents the altitudinal variation of difference in trend of the  $T_{\text{mean}}$  between the models and observation to study the under/over representation of warming or cooling rate by models and its dependence on elevation. The model and ENSEMBLE shows higher agreement with the observation at the lower elevation, but the same cannot be said in case of high elevation grid points. Though the ENSEMBLE under simulates the observed temperature magnitude in form of cold bias, but the rate of its long-term increase is over simulated as is clearly seen in Fig. 15 and further in Table 2. There exists gridpoints at lower as well

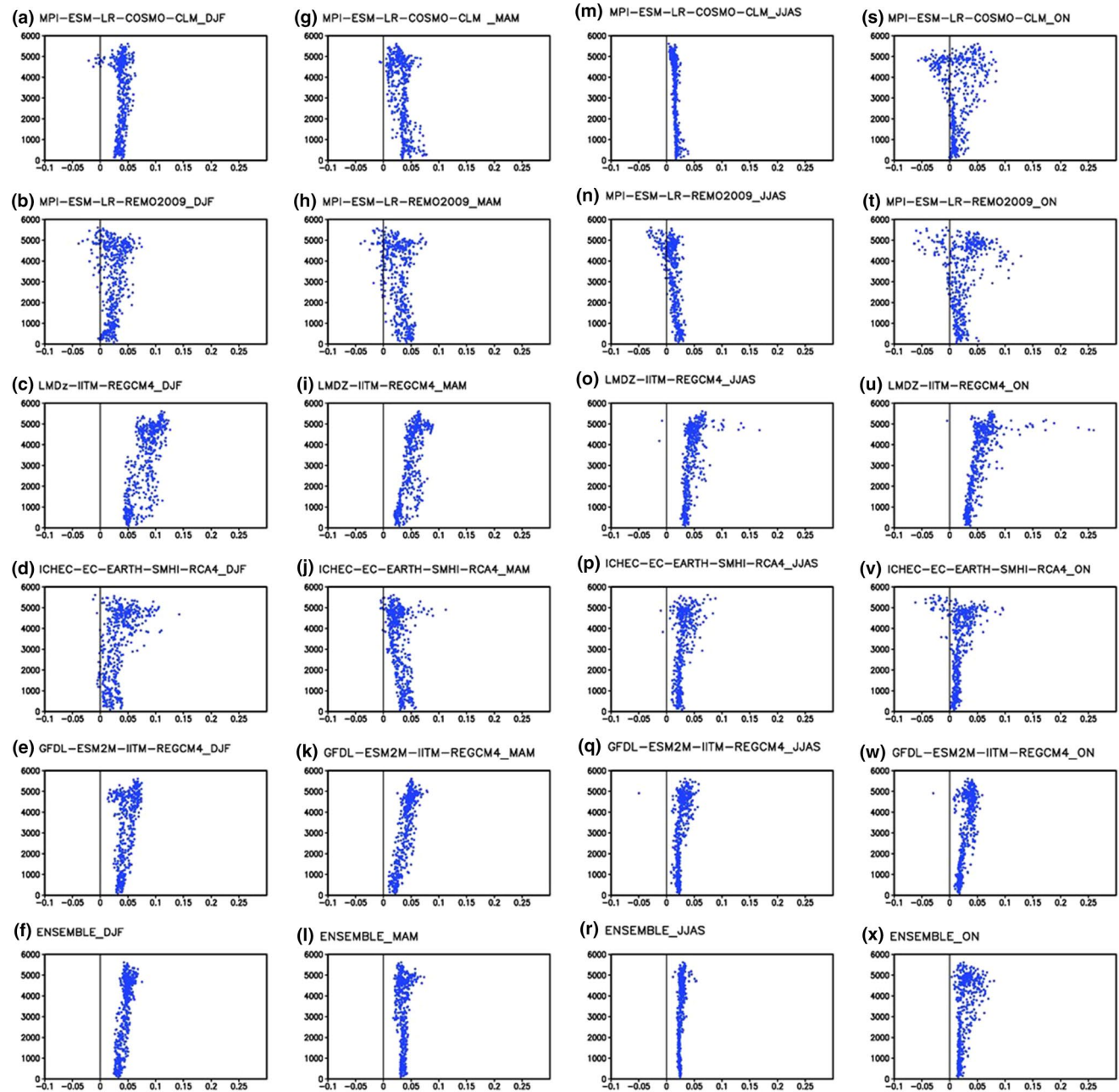


**Fig. 14** Variation in trend ( $^{\circ}\text{C}/\text{year}$ ) with elevation (m) of mean temperature,  $T_{\text{mean}}$  for different seasons for five CORDEX-SA experiments and their corresponding ENSEMBLE. First column corresponds to winter (DJF); second column corresponds to pre-monsoon (MAM), third column corresponds to monsoon (JJAS) and last column corresponds to post-monsoon (ON)

sponds to winter (DJF); second column corresponds to pre-monsoon (MAM), third column corresponds to monsoon (JJAS) and last column corresponds to post-monsoon (ON)

as at higher elevations, where the ENSEMBLE seems to show greater rate of warming than the observation, which is most pronounced during DJF. However during JJAS and ON, between 5000–5500m the ENSEMBLE seems to underestimate the rate of warming (see Table 2). Furthermore, elevation based dependence of model performance variability is seen. Very similar to observation, in the middle elevations for the ENSEMBLE there is a wide spatial

variability in the differences of trend while at the high and low end elevations the differences are found to be much smaller and similar among different grid points.

Figure 16 shows the temporal pattern of yearly  $T_{\text{mean}}$  averaged over the study region for the time period of 36 years (1970–2005) for all the models, their ENSEMBLE and their corresponding APHROTEMP 0.5. All the models and the ENSEMBLE show a consistent cold bias

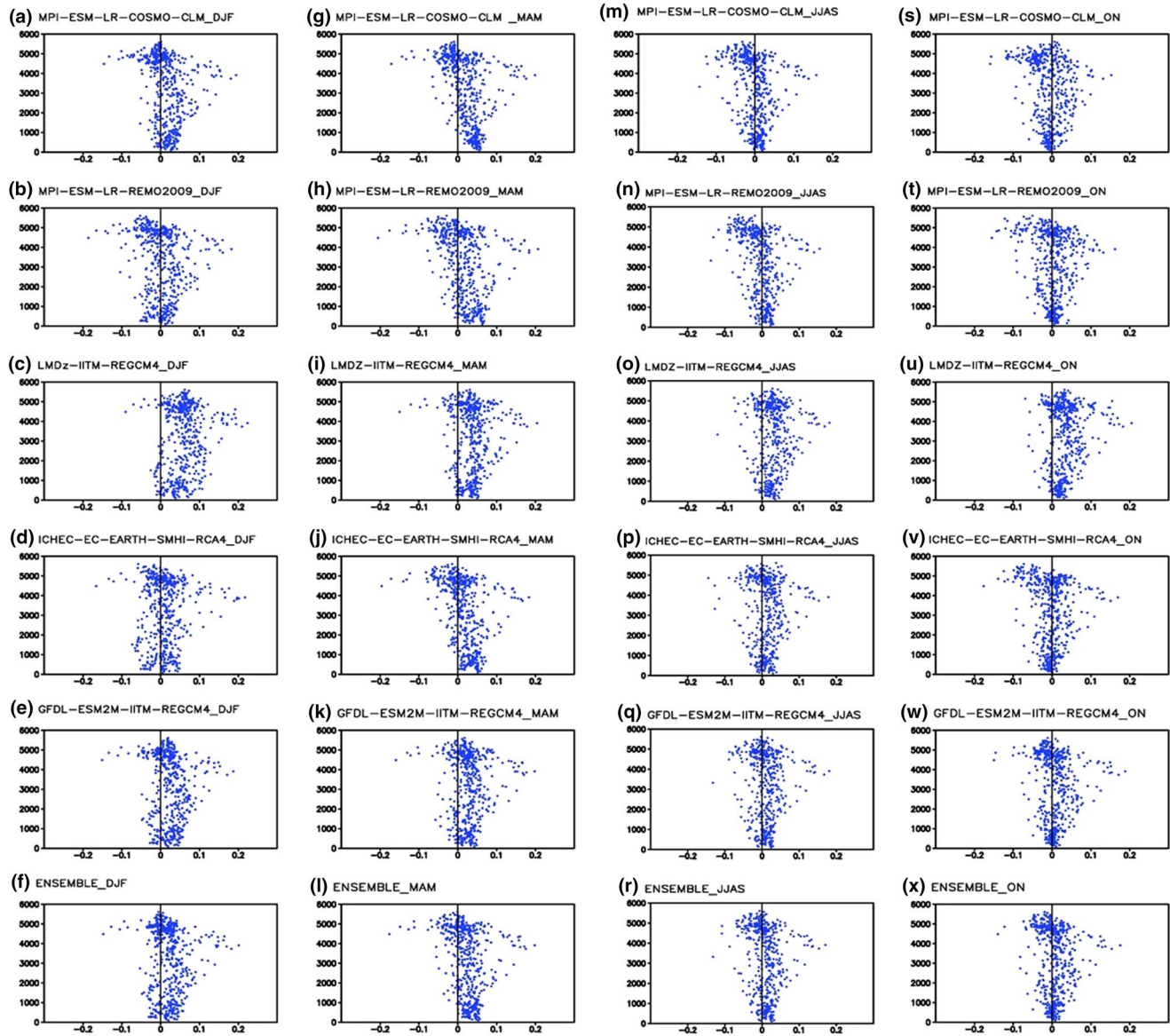


**Fig. 15** Variation of difference in trend of mean temperature,  $T_{\text{mean}}$  ( $^{\circ}\text{C}/\text{year}$ ) with elevation of five CORDEX-SA experiments and their ENSEMBLE from corresponding APHROTEMP 0.5 for different

seasons. First column corresponds to winter (DJF); second column corresponds to pre-monsoon (MAM), third column corresponds to monsoon (JJAS) and last column corresponds to post-monsoon (ON)

over the time irrespective of the season which further affirms the findings made earlier in Fig. 4. Only for the experiment MPI-ESM-LR-COSMO-CLM the range of  $T_{\text{mean}}$  values (DJF:  $-6.75$  to  $-2.7^{\circ}\text{C}$ ; MAM:  $3.5$ – $7.2^{\circ}\text{C}$ ; JJAS:  $11.4$ – $12.7^{\circ}\text{C}$ ; ON:  $2.1$ – $4.5^{\circ}\text{C}$ ) over the study period is closer to the APHROTEMP 0.5 line to a moderate extent (DJF:  $-0.25$  to  $2.4^{\circ}\text{C}$ ; MAM:  $8.5$ – $11.2^{\circ}\text{C}$ ; JJAS:  $15.7$ – $17^{\circ}\text{C}$ ; ON:  $7.2$ – $9.5^{\circ}\text{C}$ ). We also noticed that yearly variability is least during JJAS—a seasonal behaviour which seems to be well reflected in models also.

The uncertainty among the experiments is presented in Fig. 17 which shows the spatial distribution of ensemble

spread in  $T_{\text{mean}}$  as standard deviation among the five CORDEX-SA experiments at each grid for respective seasons. Here we can see that the uncertainty between the models is largest in the western Himalayan region and smallest in eastern Himalayan region. Besides spatial variation in the model uncertainty there seems to be a seasonal dependence also. Disagreement between the models is highest in MAM, where as it is lowest in JJAS and ON indicating a higher degree of reliability in the model simulations during these seasons.

The climatological performance in simulating seasonal  $T_{\text{mean}}$  by five CORDEX-SA experiments and their

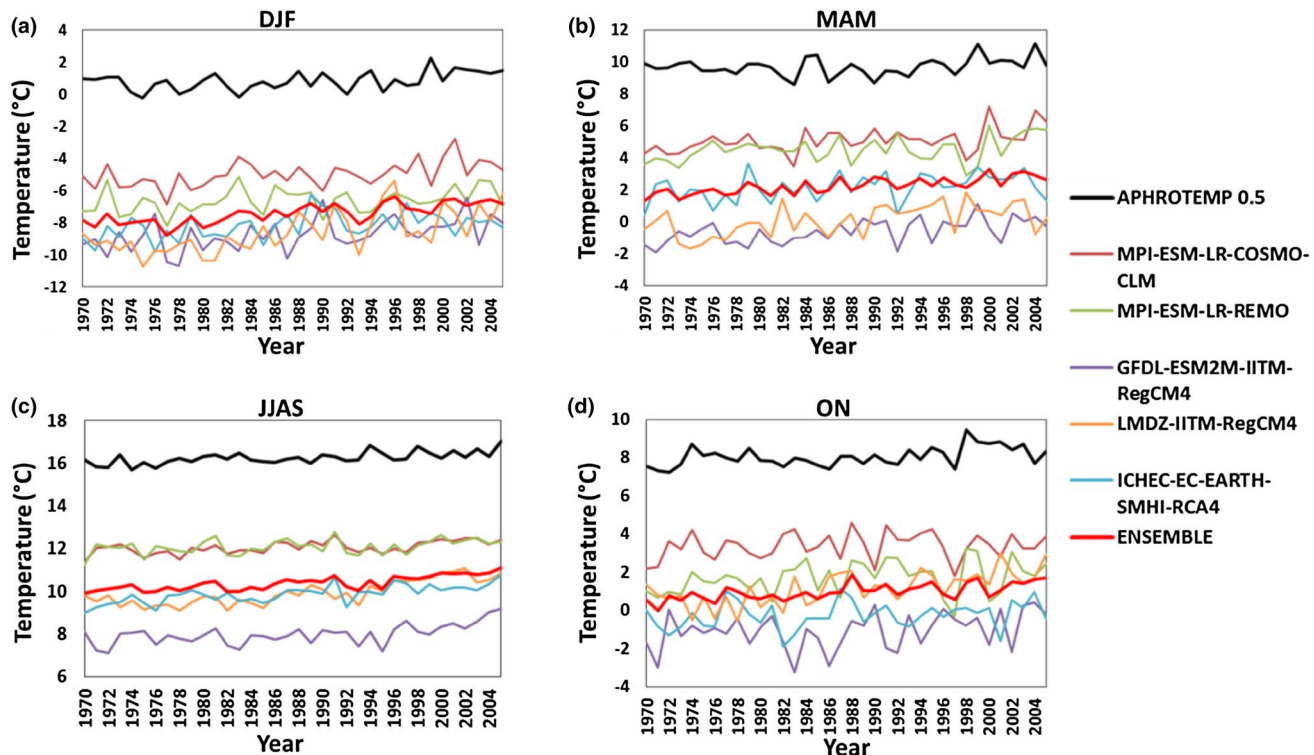


**Fig. 16** Time series of seasonal mean temperature,  $T_{\text{mean}}$  ( $^{\circ}\text{C}$ ) of five CORDEX-SA experiments, their ENSEMBLE and the corresponding observation averaged over the study region

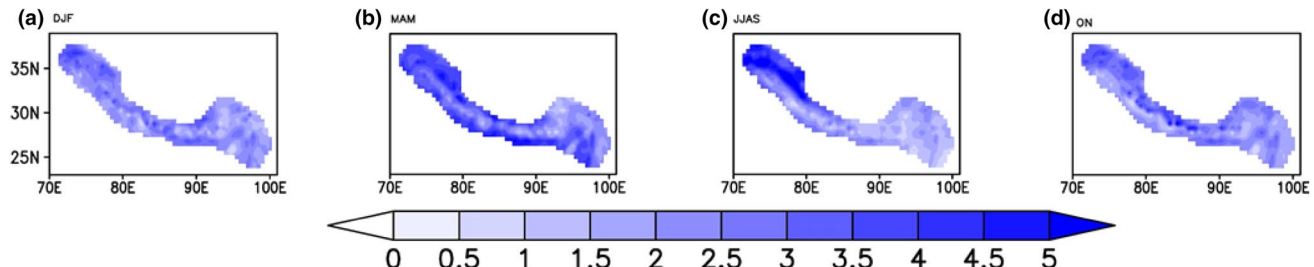


**Fig. 17** Spatial distribution of ensemble spread in mean temperature,  $T_{\text{mean}}$  (as standard deviation,  $^{\circ}\text{C}$ ) among the five CORDEX-SA experiments for respective seasons

ENSEMBLE against corresponding observation is presented in Fig. 18. It shows the area and time averaged APHROTEMP 0.5 value along with  $\pm 3$  standard deviation (over 1970–2005) from mean. All the models and hence the ENSEMBLE highly underestimates the  $T_{\text{mean}}$  climatology values as none of the models lie within  $\pm 3$  standard deviation of APHROTEMP 0.5. Compared with other experiments, COSMO-CLM and REMO lie closer to observation line though they too carry a very large cold bias.

In Fig. 19, it is seen that the grid to grid variation in the  $T_{\text{mean}}$  values is very consistently and skilfully captured by the present set of models in all the seasons throughout the period 1970–2005. This is primarily due to the

representation of fine-scale topography in the RCMs (Giorgi et al. 1994; Noguer et al. 1998; Pal et al. 2007). The orographic feedbacks in the near surface atmosphere seems to be well simulated by the models. Though the magnitude of temperature is not correctly represented by the models which we found earlier from different analyses, but its spatial variation in the complex topographic setting of the Himalayan region is very well captured indicated by a very high correlation value of greater than 0.9 in all seasons.

The normalised Taylor diagram is presented in Fig. 20 which shows the spatial pattern of errors in models along with their amplitude and spread between the models which can be inferred from closeness of model dots. Different

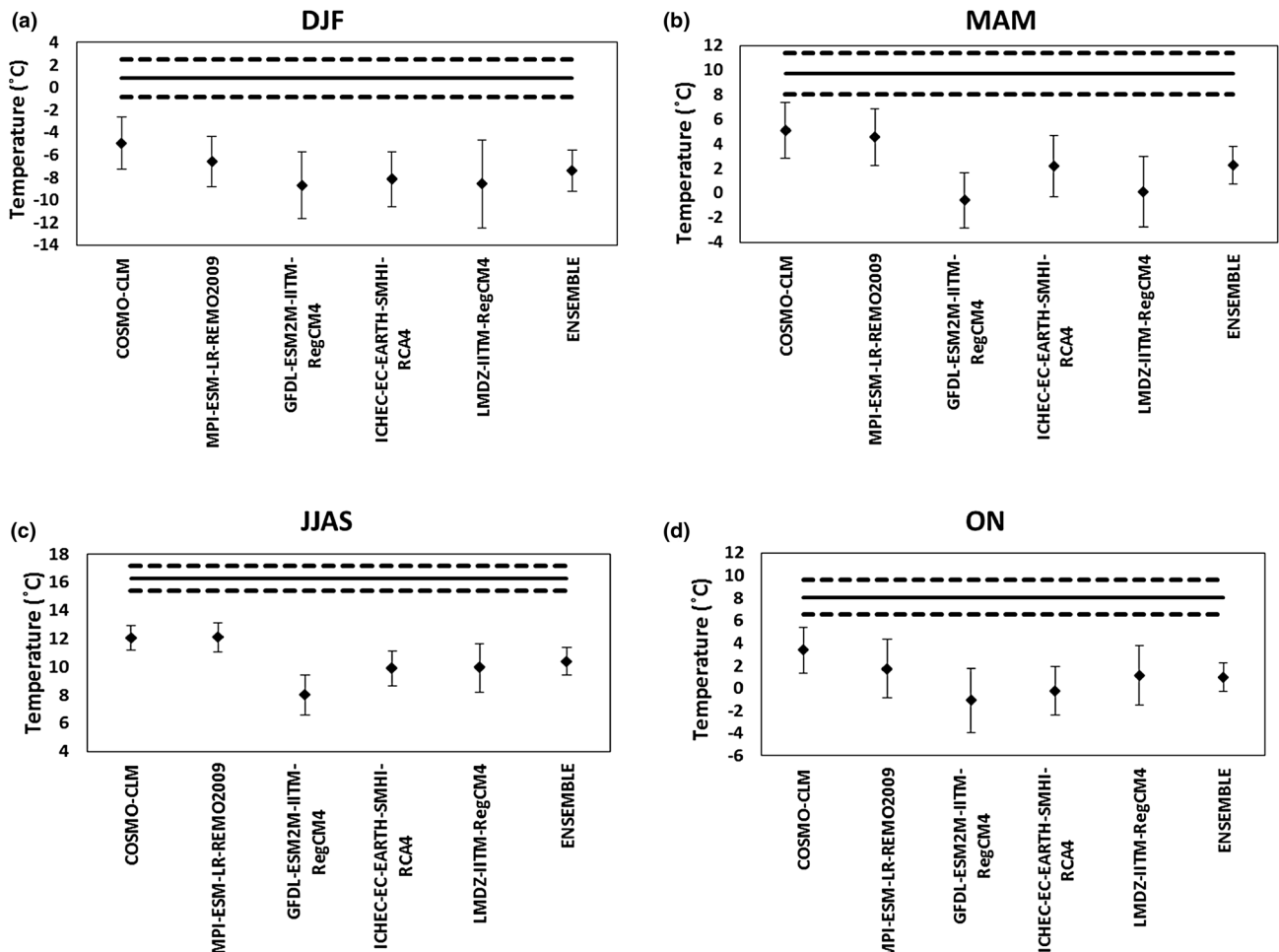


**Fig. 18** Mean temperature,  $T_{\text{mean}}$  ( $^{\circ}\text{C}$ ) climatology of five CORDEX-SA experiments, their ENSEMBLE and corresponding APHROTEMP 0.5 averaged over the study region and during 1970–2005. The *thick black line* denotes the mean temperature,  $T_{\text{mean}}$  ( $^{\circ}\text{C}$ )

models behave differently due to their varying physics, forcings and other factors but they all show a very high correlation with observation (more than 0.9) for all models and all seasons which found in previous analysis also. This implies that in spite of differences in the models, they simulate the temperature distribution quite realistically. Further, due to the lack of moisture during DJF, the dry atmospheric conditions in all models tends to drive their different model physics in a similar manner unlike in JJAS where moisture-temperature interplay comes in the model environment. Thus during DJF correlation patterns are higher as well as similar in magnitude which was also seen previously in Fig. 19. Normalised RMSE values of models, which gives a measure of bias from observation, lie below 0.6. The distance of the models from the reference black dot (APHROTEMP 0.5) represents the overall closeness of the different model with the observation. Spatial variability in the model can be inferred from the standard deviation

of the APHROTEMP 0.5, the *dashed lines* represent the  $\pm 3$  standard deviation from it. The *dots* represents the mean climatology value of each experiment and the associated *error bars* are the  $\pm 3$  standard deviation

which is in this case comparable with the observation though slightly on the higher side.

Figure 21 describes the probability distribution of climatological values as normally fitted probability distribution curve or PDF. As discussed in the  $T_{\text{mean}}$  model climatology (Fig. 3), almost all the models exhibit cold bias in all the 4 seasons, as the mean (vertical line) of the distribution of ENSEMBLE (red line) lies left to that of the mean of the observation (black line). The spread of curve represents the spatial variability. Here, the wider curve of models indicates greater spatial variability in simulated temperature than that of the observation. High spatial variability in the models is also found as discussed before (refer Fig. 6). The variability in the temperature increases with increase in elevation, the highest variability is observed at around 4000–6000 m which contributes to the ENSEMBLE's overall variability seen in its distribution. Moreover, the variability is least in case of JJAS season (a narrower

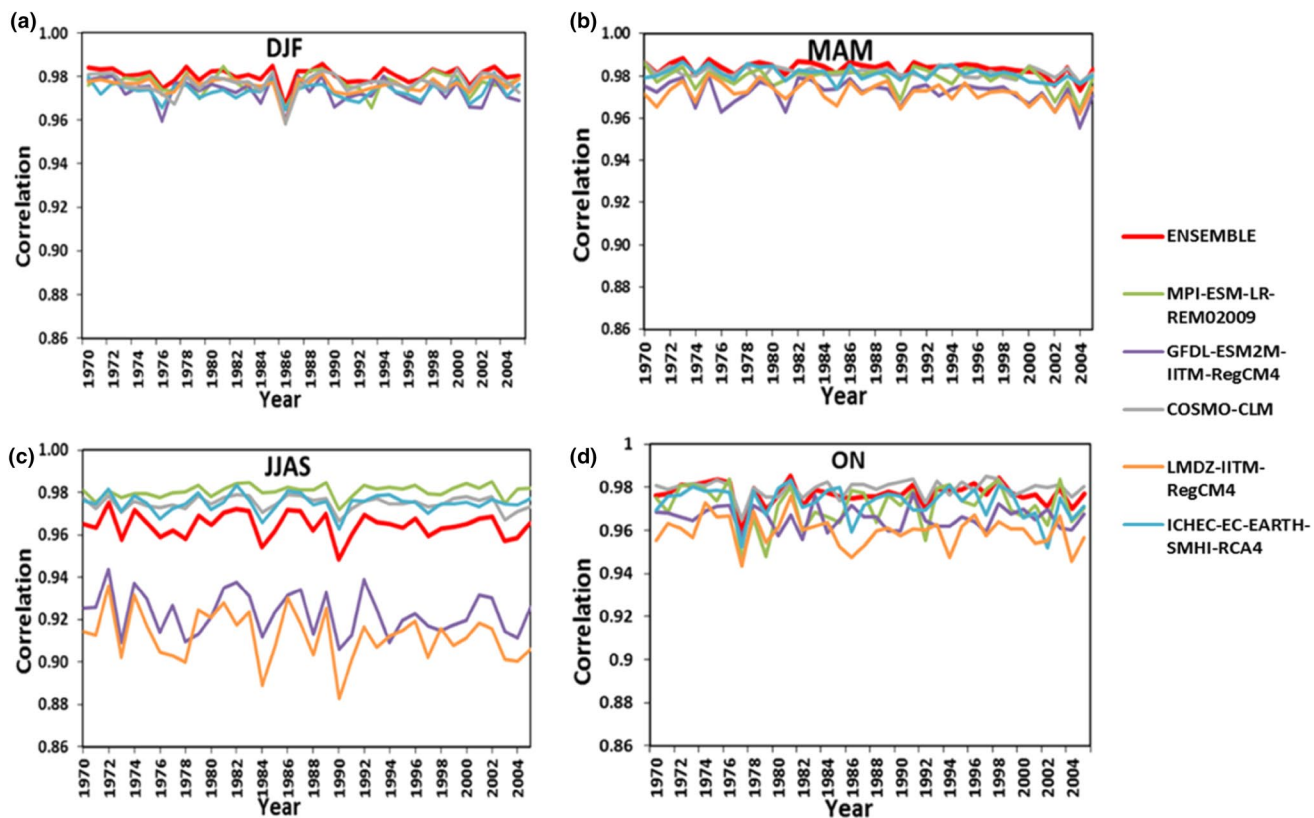


**Fig. 19** Spatial correlation of mean temperature,  $T_{\text{mean}}$  of five CORDEX-SA experiments and their ENSEMBLE with corresponding observation, APHROTEMP 0.5. for different seasons

curve) compared with other seasons. This is observed in case of models as well as APHROTEMP which shows that the models are able to capture the seasonal transition in the spatial variability although the realistic variability is overestimated.

#### 4 Conclusions

The heterogeneously varying topography of the Himalayas makes the study of climatic changes over the Himalayan region a difficult task. The temperature over the Himalayan region is highly influenced by altitude, latitude and longitude (Beniston and Rebetez 1996; Wang et al. 2013). Our understanding of climate dynamics taking place in the high mountains of the Himalayas remains limited due to inadequacies in the observational datasets (Rangwala and Miller 2012). This underlines the importance of applying climate models in studying the dynamics of atmosphere over such regions. Moreover, there exists underlying uncertainties between models and biases in them which further necessitates the evaluation of such shortcomings in the simulations. This paper presents an assessment of performance of an ensemble of

five CORDEX-SA RCM experiments in simulating near surface mean air temperature climatology with respect to the corresponding observation, over the Himalayan region for the present climate. The skill of different models has been evaluated and its variation in spatio-temporal terms has been studied. The main findings from our study are:

- The present set of models with their skill in representing the fine scale atmospheric processes perform exceptionally well in realistically capturing the spatial distribution of  $T_{\text{mean}}$ . This is evident from very high spatial correlation value of model simulated temperature with that of observation. On the other hand, the magnitude of temperature is highly underestimated by these set of models as they have an inherent cold bias which increases with height. The cold bias in the models could be due to positive precipitation bias in RCMs which causes an enhanced snow cover, moisture and evaporation feedbacks in model environment (Kotlarski et al. 2010). Ghimire et al. (2015) in their study found an extreme wet bias in these CORDEX-SA models over Himalayan region. Haslinger et al. (2013) also found a similar behaviour in models in his study over Alpine region.

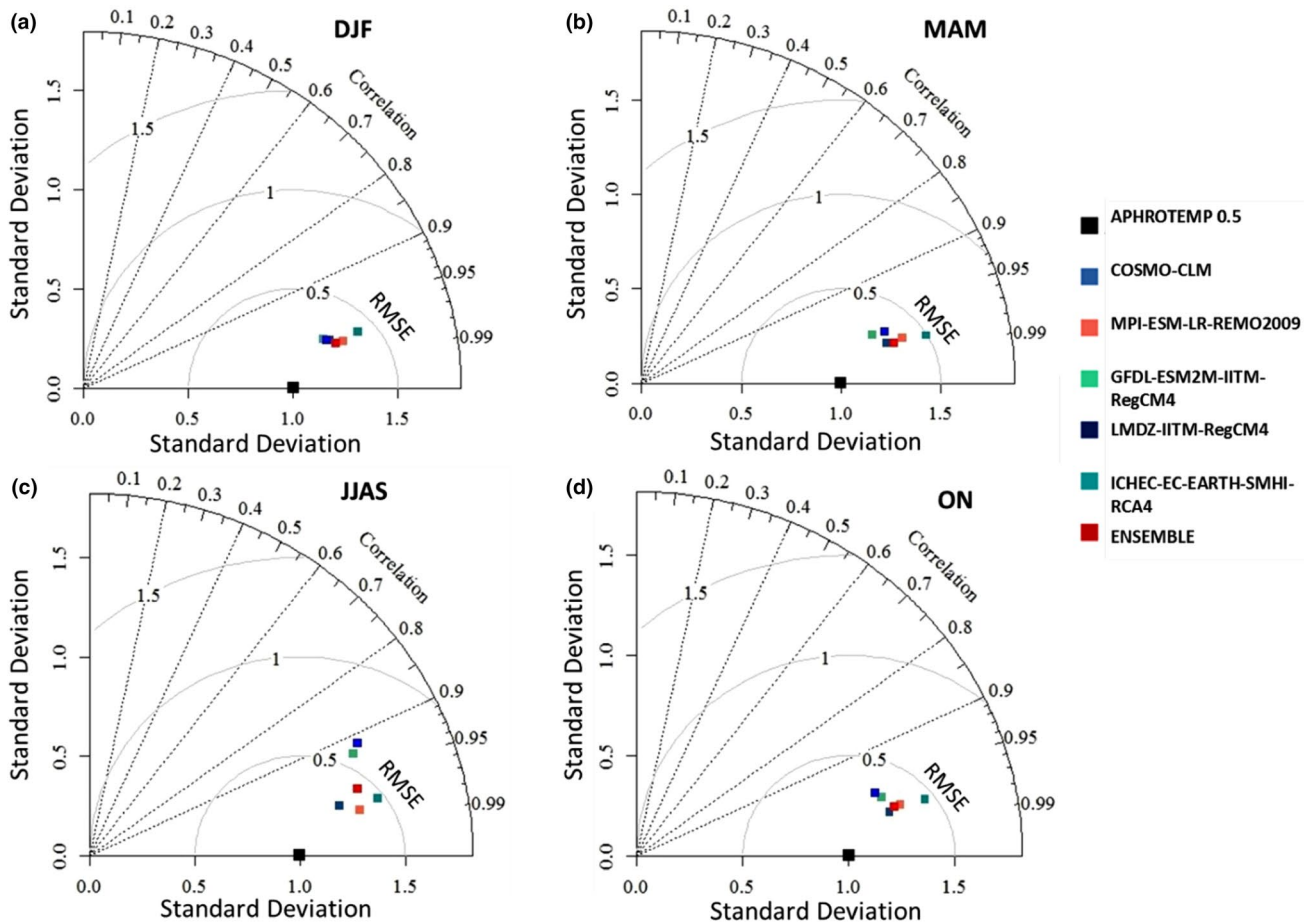


**Fig. 20** Taylor diagram showing normalized statistical comparison of seasonal mean temperature,  $T_{\text{mean}}$  ( $^{\circ}\text{C}$ ) for 1970 to 2005 of the five CORDEX-SA experiments, their ENSEMBLE and APHROTEMP 0.5

- The overall temperature bias varies between  $-6$  to  $-8^{\circ}\text{C}$  depending upon season where in DJF model shows maximum cold bias. Similar cold biases in model simulation in mountainous regions have been reported by Giorgi et al. (2004), Solomon et al. (2008), Akhtar et al. (2009), Haslinger et al. (2013) and Mishra (2015).
- Notable cold bias is seen over topographically complex northwestern Himalayas. The biases in the higher elevation regions can also get enhanced due to lack of dense observational networks and the inaccuracies and uncertainty within the observation (Nikulin et al. 2011; Walker and Diffenbaugh 2009) by which the gridded dataset has been prepared.
- Models are able to capture the phenomena of slope environmental lapse of temperature as we see that the simulated temperature decreases with heights but the lapse rate seems to be overestimated by models. This possibly further leads to an intensification of cold bias at high altitudes.
- A mixed pattern of  $T_{\text{mean}}$  trend is simulated by the CORDEX-SA models. Although a warming trend is found in

general across the study region, some models also show a cooling to low warming rate over few patches of Karakoram and northeast Himalaya. In spite of underestimation in simulated temperature and the intensification of cold bias at higher elevations the models show a greater rate of warming throughout entire altitudinal stretch of study region. During DJF the rate of warming gets even higher at high altitudes. During JJAS, the models quite realistically simulates a reduced variability compared with other seasons. This could be due to predominant role of moisture controlled thermodynamics of atmosphere which is largely unchanged during this season on an inter-annual time scale.

- The models seem to be more variable spatially at the higher altitudes which is seen in terms of a more variable climatology and trend of temperature along with their associated biases. Amplification of temperature variability at high altitude could be due to the variation in surface energy balance, temperature-cryosphere feedback and topography, induced by the lower temperature at high altitude (Ohmura 2012).

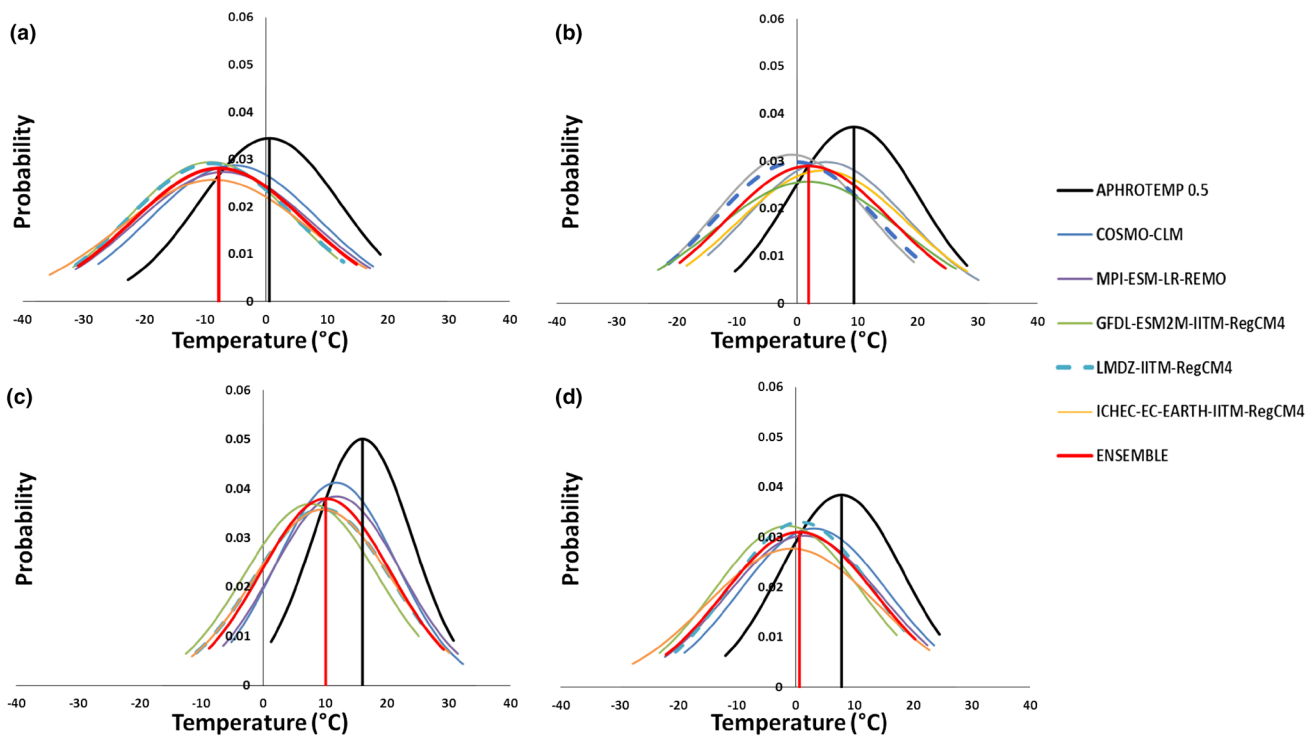


**Fig. 21** Probability distribution function (as fitted Gaussian distribution) of the spatially distributed seasonal mean temperature,  $T_{\text{mean}}(\text{°C})$  values for 1970–2005 for five CORDEX-SA experiments

Nonetheless, it is not reasonable to evaluate the performance of models with a single observational dataset, because we have found differences even in various observational datasets. The study therefore, also point towards a need for an improvement in the gridded observational datasets over mountainous region to reduce the uncertainties in the model simulations and its assessment. In summary, the performance of models varies with each other and individually with space, time and season. However a large cold bias in general consistently occurs which can be dealt with suitable bias correction methods if they are to be used in future for climate impact studies. Addition analysis in detail is required with a similar study using other variables like cloud fraction, moisture, snow cover, radiation flux etc. in order to establish the specific mechanisms and processes responsible for a particular weakness in model. Such study could not be carried out as these variables are currently unavailable for all the models we considered here but it is expected to be publicly available in near future. Nonetheless, the study documents at one place the performance of multiple RCMs as CORDEX project is in focus across the world and is considered to be a major source of information for future climate projections and impact studies. The present study along with other studies in CORDEX framework therefore could be beneficial in designing future course of actions under

and their corresponding ENSEMBLE and APHROTEM 0.5. The vertical lines correspond to the mean of the distribution

CORDEX, in selecting particular models for impact studies or even their improvement.

**Acknowledgements** The authors thank the World Climate Research Programme's Working Group on Regional Climate, the Working Group on Coupled Modelling which formerly coordinated CORDEX. We are also grateful to the climate modeling groups (listed in Table 1) for producing and making available their model output. The authors also thank the Earth System Grid Federation (ESGF) infrastructure and the Climate Data Portal at Center for Climate Change Research (CCCR), Indian Institute of Tropical Meteorology, India for provision of CORDEX South Asia data.. Also, we thank Ministry of the Environment, Japan's APHRODITE water resources project, supported by the Environment Research and Technology Development Fund for provision of APHROTEM data and Climatic Research Unit, University of East Anglia, United Kingdom for providing CRU data on their respective websites. The UDWand NCEP data is provided by the NOAA/OAR/ESRL PSD, Boulder, Colorado, USA, on their website at <http://www.esrl.noaa.gov/psd/>. We acknowledge the comments and suggestions of two anonymous reviewers which helped us in improving the manuscript.

## References

- Akhtar M, Ahmad N, Booij MJ (2009) Use of regional climate model simulations as input for hydrological models for the Hindu-kush–Karakorum–Himalaya region. Hydrol Earth Syst Sci 13(7):1075–1089

- Barnett TP, Adam JC, Lettenmaier DP (2005) Potential impacts of a warming climate on water availability in snow-dominated regions. *Nature* 438(7066):303–309
- Becker AB (1997) Predicting global change impacts on mountain hydrology and ecology: integrated catchment hydrology/altitudinal gradient studies workshop report: documentation resulting from an international workshop, Kathmandu, Nepal 30 March–2 April 1996 (No. F/304.2 I5/43). International Geosphere Biosphere Programme [Stockholm]
- Beniston M (2003) Climatic change in mountain regions: a review of possible impacts. In: Climate variability and change in high elevation regions: Past, present and future. Springer, The Netherlands, pp 5–31
- Beniston M, Rebetez M (1996) Regional behavior of minimum temperatures in Switzerland for the period 1979–1993. *Theoret Appl Climatol* 53(4):231–243
- Beniston M, Diaz HF, Bradley RS (1997) Climatic change at high elevation sites: an overview. *Clim Change* 36(3–4):233–251
- Bhutiyani MR, Kale VS, Pawar NJ (2007) Long-term trends in maximum, minimum and mean annual air temperatures across the Northwestern Himalaya during the twentieth century. *Clim Change* 85(1–2):159–177
- Bond-Lamberty B, Thomson A (2010) Temperature-associated increases in the global soil respiration record. *Nature* 464(7288):579–582
- Chen B, Chao WC, Liu X (2003) Enhanced climatic warming in the Tibetan Plateau due to doubling CO<sub>2</sub>: a model study. *Clim Dyn* 20(4):401–413
- Daly C (2006) Guidelines for assessing the suitability of spatial climate data sets. *Int J Climatol* 26(6):707–721
- Dash SK, Jenamani RK, Kalsi SR, Panda SK (2007) Some evidence of climate change in twentieth-century India. *Clim Change* 85(3–4):299–321
- Diaz HF, Bradley RS (1997) Temperature variations during the last century at high elevation sites. In: Climatic change at high elevation sites. Springer, The Netherlands, pp 21–47
- Diaz HF, Grosjean M, Graumlich L (2003) Climate variability and change in high elevation regions: past, present and future. Springer, The Netherlands, pp 1–4
- Dimri AP (2009) Impact of subgrid scale scheme on topography and landuse for better regional scale simulation of meteorological variables over the western Himalayas. *Climate dynamics* 32(4):565–574
- Dimri AP, Dash SK (2012) Wintertime climatic trends in the western Himalayas. *Clim Change* 111(3–4):775–800
- Diodato N, Bellocchi G, Tartari G (2012) How do Himalayan areas respond to global warming? *Int J Climatol* 32(7):975–982
- Dobler A, Ahrens B (2008) Precipitation by a regional climate model and bias correction in Europe and South Asia. *Meteorologische Zeitschrift* 17(4):499–509
- Du M, Kawashima S, Yonemura S, Zhang X, Chen S (2004) Mutual influence between human activities and climate change in the Tibetan Plateau during recent years. *Glob Planet Change* 41(3):241–249
- Duncan J, Dash J, Atkinson PM (2015) Elucidating the impact of temperature variability and extremes on cereal croplands through remote sensing. *Glob Change Biol* 21(4):1541–1551
- Dunne JP, John JG, Adcroft AJ, Griffies SM, Hallberg RW, Shevliakova E, Zadeh N (2012) GFDL's ESM2 global coupled climate-carbon Earth System Models. Part I: physical formulation and baseline simulation characteristics. *J Clim* 25(19):6646–6665
- Ensor LA, Robeson SM (2008) Statistical characteristics of daily precipitation: comparisons of gridded and point datasets. *J Appl Meteorol Climatol* 47(9):2468–2476
- Evans JP (2011) CORDEX—an international climate downscaling initiative. In 19th International Congress on Modelling and Simulation, Perth, Australia, 12–16 December 2011
- Fan F, Bradley RS, Rawlins MA (2014) Climate change in the north-eastern US: regional climate model validation and climate change projections. *Clim Dyn* 43(1–2):145–161
- Fan F, Bradley RS, Rawlins MA (2015) Climate change in the Northeast United States: an analysis of the NARCCAP multimodel simulations. *J Geophys Res Atmos* 120(2):10569–10592. doi:[10.1002/2015JD023073](https://doi.org/10.1002/2015JD023073)
- Fernández J, Fita L, García-Díez M, Gutiérrez J M (2010) WRF sensitivity simulations on the CORDEX African domain. In EGU General Assembly Conference Abstracts (vol 12, p 9701)
- Forsythe N, Blenkinsop S, Fowler HJ (2014) Exploring objective climate classification for the Himalayan arc and adjacent regions using gridded data sources. *Earth Syst Dyn Discuss* 5(2)
- Fowler HJ, Archer DR (2005) Hydro-climatological variability in the Upper Indus Basin and implications for water resources. *Reg Hydrol Impacts Clim Change Impact Assess Dec Mak* 295:131–138
- Fowler HJ, Archer DR (2006) Conflicting signals of climatic change in the Upper Indus Basin. *J Clim* 19(17):4276–4293
- Gao XJ, Li DL, Zhao ZC, Giorgi F (2003) Climate change due to greenhouse effects in Qinghai-Xizang Plateau and along the Qianghai-Tibet Railway. *Plateau Meteorol* 22(5):458–463
- Gautam R, Hsu NC, Lau KM, Tsay SC, Kafatos M (2009) Enhanced pre-monsoon warming over the Himalayan-Gangetic region from 1979 to 2007. *Geophys Res Lett* 36:L07704. doi:[10.1029/2009GL037641](https://doi.org/10.1029/2009GL037641)
- Globally EO, Abiodun BJ, Tadross MA, Hewitson BC, Gutowski WJ (2011) The coupling of cloud base height and surface fluxes: a transferability intercomparison. *Theoret Appl Climatol* 106(1–2):189–210
- Ghimire S, Choudhary A, Dimri AP (2015) Assessment of the performance of CORDEX-South Asia experiments for monsoonal precipitation over the Himalayan region during present climate: Part I. *Clim Dyn*. doi:[10.1007/s00382-015-2747-2](https://doi.org/10.1007/s00382-015-2747-2)
- Giorgi F, Jungclaus J, Reick CH, Legutke S, Bader J, Böttinger M, Stevens B (2013) Climate and carbon cycle changes from 1850 to 2100 in MPI-ESM simulations for the Coupled Model Intercomparison Project phase 5. *J Adv Model Earth Syst* 5(3):572–597
- Giorgi F, Bates GT (1989) The climatological skill of a regional model over complex terrain. *Mon Weather Rev* 117(11):2325–2347
- Giorgi F, Shields Brodeur C, Bates GT (1994) Regional climate change scenarios over the US produced with a nested regional climate model. *J Clim* 7(3):375–399
- Giorgi F, Bi X, Pal JS (2004) Mean, interannual variability and trends in a regional climate change experiment over Europe. I. Present-day climate (1961–1990). *Clim Dyn* 22(6–7):733–756
- Giorgi F, Diffenbaugh NS, Gao XJ, Coppola E, Dash SK, Frumento O, Sylla B (2008) The regional climate change hyper-matrix framework. *Eos Trans Am Geophys Union* 89(45), 445–446
- Giorgi F, Jones C, Asrar GR (2009) Addressing climate information needs at the regional level: the CORDEX framework. *World Meteorol Org Bull* 58(3):175
- Giorgi F, Coppola E, Solmon F, Mariotti L, Sylla MB, Bi X, Brankovic C (2012) RegCM4: model description and preliminary tests over multiple CORDEX domains. *Clim Res* 2(7)
- Hall G (2015) Pearson's correlation coefficient. [http://www.hep.ph.ic.ac.uk/~hallg/UG\\_2015/Pearsons.pdf](http://www.hep.ph.ic.ac.uk/~hallg/UG_2015/Pearsons.pdf). Accessed 5 July 2015
- Hamada A, Arakawa O, Yatagai A (2011) An automated quality control method for daily rain-gauge data. *Glob Environ Res* 15(2):183–192

- Hamlet AF, Lettenmaier DP (2005) Production of temporally consistent gridded precipitation and temperature fields for the Continental US\*. *J Hydrometeorol* 6(3):330–336
- Harris IPDJ, Jones PD, Osborn TJ, Lister DH (2014a) Updated high-resolution grids of monthly climatic observations—the CRU TS3. 10 Dataset. *Int J Climatol* 34(3):623–642
- Harris I, Jones PD, Osborn TJ, Lister DH (2014b) CRU TS3. 22: Climatic Research Unit (CRU) Time-Series (TS) Version 3.22 of high resolution gridded data of month-by-month variation in climate (Jan. 1901–Dec. 2013). doi:[10.5285/18BE23F8-D252-482D-8AF9-5D6A2D40990C](https://doi.org/10.5285/18BE23F8-D252-482D-8AF9-5D6A2D40990C)
- Haslinger K, Anders I, Hofstätter M (2013) Regional climate modelling over complex terrain: an evaluation study of COSMO-CLM hindcast model runs for the Greater Alpine Region. *Clim Dyn* 40(1–2):511–529
- Hazeleger W, Wang X, Severijns C, Štefănescu S, Bintanja R, Sterl A, van der Wiel K (2012) EC-Earth V2. 2: description and validation of a new seamless earth system prediction model. *Clim Dyn* 39(11):2611–2629
- He Y, Lu A, Zhang Z, Pang H, Zhao J (2005) Seasonal variation in the regional structure of warming across China in the past half century. *Clim Res* 28(3):213–219
- Hewitt K (2005) The Karakoram anomaly? Glacier expansion and the ‘elevationeffect’, Karakoram Himalaya. *Mt Res Dev* 25(4):332–340
- Hofstra N, Haylock M, New M, Jones P, Frei C (2008) Comparison of six methods for the interpolation of daily, European climate data. *J Geophys Res* 113:D21110. doi:[10.1029/2008JD010100](https://doi.org/10.1029/2008JD010100)
- Hofstra N, New M, McSweeney C (2010) The influence of interpolation and station network density on the distributions and trends of climate variables in gridded daily data. *Clim Dyn* 35(5):841–858
- Immerzeel W (2008) Historical trends and future predictions of climate variability in the Brahmaputra basin. *Int J Climatol* 28(2):243
- Immerzeel WW, Droogers P, De Jong SM, Bierkens MFP (2009) Large-scale monitoring of snow cover and runoff simulation in Himalayan river basins using remote sensing. *Remote Sens Environ* 113(1):40–49
- IPCC (2007) Climate change 2007—the physical science basis: Working group I contribution to the fourth assessment report of the IPCC (vol 4). Cambridge University Press, Cambridge
- IPCC (2014). Climate change 2013: the physical science basis: Working Group I contribution to the Fifth assessment report of the Intergovernmental Panel on Climate Change. Cambridge University Press, Cambridge
- Jomelli V, Pech VP, Chochillon C, Brunstein D (2004) Geomorphic variations of debris flows and recent climatic change in the French Alps. *Clim Change* 64(1–2):77–102
- Jones PD, Mann ME (2004) Climate over past millennia. *Rev Geophys* 42:RG2002. doi:[10.1029/2003RG000143](https://doi.org/10.1029/2003RG000143)
- Jones C, Giorgi F, Asrar G (2011) The Coordinated Regional Downscaling Experiment: CORDEX, an international downscaling link to CMIP5. *CLIVAR Exch* 16(2):34–40
- Kalnay E, Cai M (2003) Impact of urbanization and land-use change on climate. *Nature* 423(6939):528–531
- Kalnay E, Kanamitsu M, Kistler R, Collins W, Deaven D, Gandin L, Zhu (1996) The NCEP/NCAR 40-year reanalysis project. *Bull Am Meteorol Soc* 77(3):437–471
- Kang S, Zhang Y, Qin D, Ren J, Zhang Q, Grigholm B, Mayewski PA (2007) Recent temperature increase recorded in an ice core in the source region of Yangtze River. *Chin Sci Bullet* 52(6):825–831
- Khattak MS, Babel MS, Sharif M (2011) Hydro-meteorological trends in the upper Indus River basin in Pakistan. *Clim Res* 46(2):103
- Kotlarski S, Paul F, Jacob D (2010) Forcing a distributed glacier mass balance model with the regional climate model REMO. Part I: climate model evaluation. *J Clim* 23(6):1589–1606
- Kotlarski S, Bosshard T, Lüthi D, Pall P, Schär C (2012) Elevation gradients of European climate change in the regional climate model COSMO-CLM. *Clim Chang* 112(2):189–215
- Krishnamurti TN, Mishra AK, Simon A, Yatagai A (2009) Use of a dense rain-gauge network over India for improving blended TRMM products and downscaled weather models. *Meteorol J Part 2* 87:393–412
- Kulkarni A, Patwardhan S, Kumar KK, Ashok K, Krishnan R (2013) Projected climate change in the Hindu Kush–Himalayan region by using the high-resolution regional climate model PRECIS. *Mt Res Dev* 33(2):142–151
- Kumar KR, Sahai AK, Kumar KK, Patwardhan SK, Mishra PK, Revadekar JV, Pant GB (2006) High-resolution climate change scenarios for India for the 21st century. *Curr Sci* 90(3):334–345
- Kumar P, Wiltshire A, Mathison C, Ashraf S, Ahrens B, Lucas-Picher P, Christensen JH, Gobiet A, Saeed F, Hageman S, Jacob D (2013) Downscaled climate change projections with uncertainty assessment over India using a high resolution multi-model approach. *Sci Total Environ* 468:18–30
- Lau WK, Kim MK, Kim KM, Lee WS (2010) Enhanced surface warming and accelerated snow melt in the Himalayas and Tibetan Plateau induced by absorbing aerosols. *Environ Res Lett* 5(2):025204
- Li D-L, Wu Q-B, Tang M-C (2005) The time-space variety characteristics of the surface temperature over the Qinghai-Tibet plateau [J]. *Sci Technol Rev* 1:004
- Liu X, Chen B (2000) Climatic warming in the Tibetan Plateau during recent decades. *Int J Climatol* 20(14):1729–1742
- Liu XD, Hou P (1998) Relationship between the climatic warming over the Qinghai-Xizang Plateau and its surrounding areas in recent 30 years and the elevation. *Plateau Meteorol* 17(3):245–249 (in Chinese with English Abstract)
- Liu X, Cheng Z, Yan L, Yin ZY (2009) Elevation dependency of recent and future minimum surface air temperature trends in the Tibetan Plateau and its surroundings. *Glob Planet Change* 68(3):164–174
- Lobell DB, Bonfils C, Duffy PB (2007) Climate change uncertainty for daily minimum and maximum temperatures: a model intercomparison. *Geophys Res Lett* 34:L05715. doi:[10.1029/2006GL028726](https://doi.org/10.1029/2006GL028726)
- Lu A, He Y, Zhang Z, Pang H, Gu J (2004) Regional structure of global warming across China during the twentieth century. *Clim Res* 27(3):189–195
- Lu A, Pang D, Ge J, He Y, Pang H, Yuan L (2006) Effect of landform on seasonal temperature structures across China in the past 52 years. *J Mt Sci* 3(2):158–167
- Lu A, Kang S, Li Z, Theakstone WH (2010) Altitude effects of climatic variation on Tibetan Plateau and its vicinities. *J Earth Sci* 21:189. doi:[10.1007/s12583-010-0017-0](https://doi.org/10.1007/s12583-010-0017-0)
- Madhura RK, Krishnan R, Revadekar JV, Mujumdar M, Goswami BN (2015) Changes in western disturbances over the Western Himalayas in a warming environment. *Clim Dyn* 44(3–4):1157–1168
- Matsuura K, Willmott C (2009) Terrestrial air temperature and precipitation: 1900–2008 gridded monthly time series (V2. 01). <http://climate.goeg.udel.edu>
- Mishra V (2015) Climatic uncertainty in Himalayan water towers. *J Geophys Res Atmos* 120(7):2689–2705
- Mote P, Brekke L, Duffy PB, Maurer E (2011). Guidelines for constructing climate scenarios. *Eos* 92(31):257–258
- New M, Lister D, Hulme M, Makin I (2002) A high-resolution data set of surface climate over global land areas. *Clim Res* 21(1):1–25

- Nieuwolt S (1977) Tropical climatology. An introduction to the climates of the low latitudes. Wiley, Oxford
- Nikulin G, Kjellström E, Hansson ULF, Strandberg G, Ullerstig A (2011) Evaluation and future projections of temperature, precipitation and wind extremes over Europe in an ensemble of regional climate simulations. *Tellus A* 63(1):41–55
- Noguer M, Jones R, Murphy J (1998) Sources of systematic errors in the climatology of a regional climate model over Europe. *Clim Dyn* 14(10):691–712
- Ohmura A (2012) Enhanced temperature variability in high-altitude climate change. *Theoret Appl Climatol* 110(4):499–508
- Overpeck JT, Meehl GA, Bony S, Easterling DR (2011) Climate data challenges in the 21 st century. *Science* (Washington), 331(6018):700–702
- Pal JS, Giorgi F, Bi X, Elguindi N, Solmon F, Rauscher SA, Ashfaq M (2007) Regional climate modeling for the developing world: the ICTP RegCM3 and RegCNET. *Bull Am Meteorol Soc* 88(9):1395–1409
- Palazzi E, Hardenberg J, Provenzale A (2013) Precipitation in the Hindu-Kush Karakoram Himalaya: observations and future scenarios. *J Geophys Res Atmos* 118(1):85–100
- Panday PK, Thibeault J, Frey KE (2015) Changing temperature and precipitation extremes in the Hindu Kush–Himalayan region: an analysis of CMIP3 and CMIP5 simulations and projections. *Int J Climatol* 35(10):3058–3077
- Pellicciotti F, Buerki C, Immerzeel WW, Konz M, Shrestha AB (2012) Challenges and uncertainties in hydrological modeling of remote Hindu Kush–Karakoram–Himalayan (HKH) basins: suggestions for calibration strategies. *Mt Res Dev* 32(1):39–50
- Pepin N, Losleben M (2002) Climate change in the Colorado Rocky Mountains: free air versus surface temperature trends. *Int J Climatol* 22(3):311–329
- Pepin NC, Lundquist JD (2008) Temperature trends at high elevations: patterns across the globe. *Geophys Res Lett* 35:L14701. doi:[10.1029/2008GL034026](https://doi.org/10.1029/2008GL034026)
- Pepin NC, Seidel DJ (2005) A global comparison of surface and free-air temperatures at high elevations. *J Geophys Res Atmos* 110(D3). doi:[10.1029/2004jd005047](https://doi.org/10.1029/2004jd005047)
- Pepin N, Bradley RS, Diaz HF, Baraer M, Caceres EB, Forsythe N, Fowler H, Greenwood G, Hashmi MZ, Liu XD, Miller LR et al (2015) Elevation-dependent warming in mountain regions of the world. Mountain Research Initiative EDW Working Group. *Nat Clim Chang* 5(5):424–430
- Perry M, Hollis D (2005) The generation of monthly gridded datasets for a range of climatic variables over the UK. *Int J Climatol* 25(8):1041–1054
- Peterson TC, Vose R, Schmoyer R, Razuvaev V (1998) Global Historical Climatology Network (GHCN) quality control of monthly temperature data. *Int J Climatol* 18(11):1169–1179
- Qin J, Yang K, Liang S, Guo X (2009) The altitudinal dependence of recent rapid warming over the Tibetan Plateau. *Clim Change* 97(1–2):321–327
- Qiu J (2008) China: the third pole. *Nat News* 454(7203), 393–396
- Rajbhandari R, Shrestha AB, Kulkarni A, Patwardhan SK, Bajracharya SR (2015) Projected changes in climate over the Indus river basin using a high resolution regional climate model (PRECIS). *Clim Dyn* 44(1–2):339–357
- Rangwala I (2013) Amplified water vapour feedback at high altitudes during winter. *Int J Climatol* 33(4):897–903
- Rangwala I, Miller JR (2012) Climate change in mountains: a review of elevation-dependent warming and its possible causes. *Clim Change* 114(3–4):527–547
- Rangwala I, Miller JR, Xu M (2009) Warming in the Tibetan Plateau: possible influences of the changes in surface water vapor. *Geophys Res Lett* 36:L06703. doi:[10.1029/2009GL037245](https://doi.org/10.1029/2009GL037245)
- Rebetz M (2004) Summer 2003 maximum and minimum daily temperatures over a 3300 m altitudinal range in the Alps. *Clim Res* 27(1):45–50
- Rummukainen M (2010) State-of-the-art with regional climate model. Wiley interdisciplinary review. *Clim Change* 1:82–96
- Ruosteenoja K, Carter TR, Jylhä K, Tuomenvirta H (2003) Future climate in world regions: an intercomparison of model-based projections for the new IPCC emissions scenarios, vol 644. Finnish Environment Institute, Helsinki
- Saeed F, Hagemann S, Jacob D (2012) A framework for the evaluation of the South Asian summer monsoon in a regional climate model applied to REMO. *Int J Climatol* 32(3):430–440
- Samuelsson P, Jones CG, Willén U, Ullerstig A, Gollvik S, Hansson U, Jansson C, Kjellström E, Nikulin G, Wyser K (2011) The Rossby Centre Regional Climate model RCA3: model description and performance. *Tellus A* 63(1):4–23
- Schmidli J, Frei C, Schär C (2001) Reconstruction of mesoscale precipitation fields from sparse observations in complex terrain. *J Clim* 14(15):3289–3306
- Schulzweida U, Kornblueh L, Quast R (2006) CDO user's guide. Climate Data Operators, Version 1(6). <https://code.zmaw.de/projects/cdo>
- Seidel DJ, Free M (2003) Comparison of lower-tropospheric temperature climatologies and trends at low and high elevation radiosonde sites. In: Diaz HF (ed) Climate variability and change in high elevation regions: past, present & future. Springer, Netherlands, pp 53–74
- Shekhar MS, Chand H, Kumar S, Srinivasan K, Ganju A (2010) Climate-change studies in the western Himalaya. *Ann Glaciol* 51(54):105–112
- Shi Y, Gao X, Zhang D, Giorgi F (2011) Climate change over the YarlungZangbo–Brahmaputra River Basin in the 21st century as simulated by a high resolution regional climate model. *Q Int* 244(2):159–168
- Shrestha AB, Aryal R (2011) Climate change in Nepal and its impact on Himalayan glaciers. *Reg Environ Change* 11(1):65–77
- Shrestha AB, Devkota LP (2010) Climate change in the Eastern Himalayas: observed trends and model projections. International Centre for Integrated Mountain Development (ICIMOD)
- Shrestha AB, Wake CP, Mayewski PA, Dibb JE (1999) Maximum temperature trends in the Himalaya and its vicinity: an analysis based on temperature records from Nepal for the period 1971–94. *J Clim* 12(9):2775–2786
- Shrestha AB, Wake CP, Dibb JE, Mayewski PA, Whitlow SI, Carmichael GR, Ferm M (2000) Seasonal variations in aerosol concentrations and compositions in the Nepal Himalaya. *Atmos Environ* 34(20):3349–3363
- Singh P, Haritashya UK, Kumar N (2008) Modelling and estimation of different components of streamflow for Gangotri Glacier basin, Himalayas/Modélisation et estimation des différentes composantes de l'écoulement fluviaile du bassin du Glacier Gangotri, Himalaya. *Hydrol Sci J* 53(2):309–322
- Snyder MA, Bell JL, Sloan LC, Duffy PB, Govindasamy B (2002) Climate responses to a doubling of atmospheric carbon dioxide for a climatically vulnerable region. *Geophys Res Lett* 29(11):9–1–9–4. doi:[10.1029/2001GL014431](https://doi.org/10.1029/2001GL014431)
- Solomon SA, Nunez MN, Cabré MF (2008) Regional climate change experiments over southern South America. I: present climate. *Clim Dyn* 30(5):533–552
- Stahl K, Moore RD, Foyer JA, Aspin MG, McKendry IG (2006) Comparison of approaches for spatial interpolation of daily air temperature in a large region with complex topography and highly variable station density. *Agric For Meteorol* 139(3):224–236
- Stewart IT (2009) Changes in snowpack and snowmelt runoff for key mountain regions. *Hydrol Process* 23(1):78–94

- Sun B, Groisman PY, Bradley RS, Keimig FT (2000) Temporal changes in the observed relationship between cloud cover and surface air temperature. *J Clim* 13(24):4341–4357
- Taylor KE (2001) Summarizing multiple aspects of model performance in a single diagram. *J Geophys Res Atmos* 106(D7):7183–7192
- Taylor KE (2005) Taylor diagram primer. [http://www.atmos.albany.edu/daes/atmclasses/atm401/spring\\_2016/ppts\\_pdfs/Taylor\\_diagram\\_primer.pdf](http://www.atmos.albany.edu/daes/atmclasses/atm401/spring_2016/ppts_pdfs/Taylor_diagram_primer.pdf)
- Thapliyal V, Kulshrestha SM (1991) Climate changes and trends over India. *Mausam* 42(4):333–338
- Thayyen RJ, Dimri AP (2014) Factors controlling slope environmental lapse rate (SELRL) of temperature in the monsoon and cold-arid glacio-hydrological regimes of the Himalaya. *Cryosphere Discuss* 8(6):5645–5686
- Tian L, Yao T, Li Z, MacClune K, Wu G, Xu B et al (2006) Recent rapid warming trend revealed from the isotopic record in Muztagata ice core, eastern Pamirs. *J Geophys Res Atmos* 111(D13). doi:[10.1029/2005JD006249](https://doi.org/10.1029/2005JD006249)
- Tse-ring K, Sharma E, Chettri N, Shrestha A (2012) Climate change vulnerability of mountain ecosystems in the Eastern Himalayas (No. id: 5000)
- Vanvyve E, Hall N, Messager C, Leroux S, Van Ypersele JP (2008) Internal variability in a regional climate model over West Africa. *Clim Dyn* 30(2–3):191–202
- Vinnikov KY, Groisman PY, Lugina KM (1990) Empirical data on contemporary global climate changes (temperature and precipitation). *J Clim* 3(6):662–677
- Vuille M, Bradley RS (2000) Mean annual temperature trends and their vertical structure in the tropical Andes. *Geophys Res Lett* 27(23):3885–3888
- Vuille M, Bradley RS, Werner M, Keimig F (2003). 20th century climate change in the tropical Andes: observations and model results. In: Climate variability and change in high elevation regions: past, present and future. Springer, The Netherlands, pp 75–99
- Walker MD, Diffenbaugh NS (2009) Evaluation of high-resolution simulations of daily-scale temperature and precipitation over the United States. *Clim Dyn* 33(7–8):1131
- Walsh JE, Jasperson WH, Ross B (1985) Influences of snow cover and soil moisture on monthly air temperature. *Mon Weather Rev* 113(5):756–768
- Wang Q, Fan X, Wang M (2014) Recent warming amplification over high elevation regions across the globe. *Clim Dyn* 43(1–2):87–101
- Wilks DS (2011). Statistical methods in the atmospheric sciences (Vol. 100). Academic Press, London
- Willmott CJ, Matsaura K (1995) Smart interpolation of annually averaged air temperature in the US. *J Appl Meteorol* 34(12):2577–2586
- Willmott CJ, Robeson SM (1995) Climatologically aided interpolation (CAI) of terrestrial air temperature. *Int J Climatol* 15(2):221–229
- Willmott CJ, Rowe CM, Philpot WD (1985) Small-scale climate maps: a sensitivity analysis of some common assumptions associated with grid-point interpolation and contouring. *Am Cartogr* 12(1):5–16
- Wiltshire AJ (2014) Climate change implications for the glaciers of the Hindu Kush, Karakoram and Himalayan region. *Cryosphere* 8(3):941–958
- Winiger MGHY, Gumpert M, Yamout H (2005) Karakorum–Hindukush–western Himalaya: assessing high-altitude water resources. *Hydrol Processes* 19(12):2329–2338
- Xie P, Chen M, Yang S, Yatagai A, Hayasaka T, Fukushima Y, Liu C (2007) A gauge-based analysis of daily precipitation over East Asia. *J Hydrometeorol* 8(3):607–626
- Xu J, Grumbine RE, Shrestha A, Eriksson M, Yang X, Wang YUN, Wilkes A (2009) The melting Himalayas: cascading effects of climate change on water, biodiversity, and livelihoods. *Conserv Biol* 23(3):520–530
- Yadav RR, Park WK, Singh J, Dubey B (2004) Do the western Himalayas defy global warming? *Geophys Res Lett* 31(17)
- Yan L, Liu X (2014) Has climatic warming over the Tibetan Plateau paused or continued in recent years. *J Earth Ocean Atmos Sci* 1:13–28
- Yang B, Achim B (2006) Temperature variations on the Tibetan Plateau during the last millennium. *Adv Clim Chang Res* 2(3):104–107
- Yang X, Zhang T, Qin D, Kang S, Qin X (2011) Characteristics and changes in air temperature and glacier's response on the north slope of Mt. Qomolangma (Mt. Everest). *Arct Antarct Alp Res* 43(1):147–160
- Yasutomi N, Hamada A, Yatagai A (2011) Development of a long-term daily gridded temperature dataset and its application to rain/snow discrimination of daily precipitation. *Glob Environ Res* 15(2):165–172
- Yatagai A, Arakawa O, Kamiguchi K, Kawamoto H, Nodzu MI, Hamada A (2009) A 44-year daily gridded precipitation dataset for Asia based on a dense network of rain gauges. *Sola* 5:137–140
- Yatagai A, Kamiguchi K, Hamada A, Arakawa O, Yasutomi N (2010) Daily precipitation analysis of using a dense network of rain gauges and satellite estimates over South Asia: quality control. In: Krishnamurti TN, Kim J, Moriyama T (eds) SPIE, remote sensing and modeling of the atmosphere, oceans, and interactions III, vol 7856. International Society for Optics and Photonics, p 785604
- Yatagai A, Kamiguchi K, Arakawa O, Hamada A, Yasutomi N, Kitoh A (2012) APHRODITE: constructing a long-term daily gridded precipitation dataset for Asia based on a dense network of rain gauges. *Bull Am Meteorol Soc* 93(9):1401–1415
- You Q, Kang S, Aguilar E, Yan Y (2008) Changes in daily climate extremes in the eastern and central Tibetan Plateau during 1961–2005. *J Geophys Res* 113:D07101. doi:[10.1029/2007JD009389](https://doi.org/10.1029/2007JD009389)
- You Q, Kang S, Pepin N, Flügel WA, Yan Y, Behrwan H, Huang J (2010) Relationship between temperature trend magnitude, elevation and mean temperature in the Tibetan Plateau from homogenized surface stations and reanalysis data. *Glob Planet Change* 71(1):124–133
- Zhang Q, Kang S, Yan Y (2006) Characteristics of spatial and temporal variations of monthly mean surface air temperature over Qinghai-Tibet Plateau. *Chin Geogr Sci* 16(4):351–358
- Zhou NF, Tu QP, Jia XL (2003) A preliminary analysis of surface and middle-upper level temperature over the northern hemisphere and the Tibetan Plateau in recent 50 years. *J Nanjing Inst Meteorol* 26(2):104–107